UNITED NATIONS UNIVERSITY
GEOTHERMAL TRAINING PROGRAMME
Orkustofnun, Grensasvegur 9,
IS-108 Reykjavik, Iceland

Reports 2012
Number 21

GEOLOGY AND HYDROTHERMAL ALTERATION OF MENENGAI GEOTHERMAL FIELD. CASE STUDY: WELLS MW-04 AND MW-05

Geoffrey Mibei
Geothermal Development Company, Ltd. – GDC
P.O. Box 17700 – 20100
Nakuru
KENYA
gmibei@yahoo.com

ABSTRACT

This study details the geological aspects of Menengai geothermal field. Surface geology is critically reviewed while the subsurface geology is reported based on the analysis of cuttings from wells MW-04 and MW-05 (has also been named MW-06). The field comprises three sectors: the Ol'rongai area, the Solai area and the Menengai caldera. The geology is divided into post-caldera, syn-caldera and pre-caldera stages while, tectonically, there are two systems: the Ol'rongai and the Solai fault systems. The faults and fractures in the Ol'rongai area have a NW direction and are older than the ones trending to the NE associated with the Solai system. Borehole data confirms that the Menengai stratigraphy is composed of a predominately trachytic lava sequence with intermittent tuffs and occasional pyroclastic layers. Different lava units are separated from each other by pyroclastic layers and sometimes by reddened soils, especially in the pre-caldera lava sequence. At shallow depths the trachyte formation consists of unconsolidated blocky lavas which are a challenge during drilling. The main hydrothermal alteration minerals are zeolites, chalcedony, quartz, pyrite, calcite, epidote, wollastonite, illite, actinolite and albite. The reservoir temperatures are between 200 and 280°C based on the presence of illite, epidote, wollastonite and actinolite. A correlation of hydrothermal alteration and fluid inclusion geothermometry indicates that the geothermal system around the caldera summit area is generally heating up.

1. INTRODUCTION

The Menengai geothermal field hosts one of the high-temperature geothermal systems in Kenya. It is located in Nakuru within the central Kenyan Rift Valley (Figure 1) and comprises the Menengai caldera, The Ol'rongai in the northwest, and parts of the Solai graben to the northeast. This report focuses mainly on the geological aspects of the Menengai caldera where 8 wells have been drilled. Wells MW-04 and MW-05 are among the exploration/production wells drilled since 2011. The two wells were drilled vertically to 2,106 and 2,200 m deep, respectively. Cuttings were sampled at 2 m interval for analysis and identification of subsurface formations, aquifers or feed zones and geothermometry. The main analytical techniques employed in this study were: binocular and petrographic microscopy, X-ray diffraction and a fluid inclusion analysis. This project report was carried out as a partial fulfilment of the six month course at the United Nations University Geothermal Training Programme (UNU-GTP).

2. EXPLORATION HISTORY OF THE MENENGAI GEOTHERMAL FIELD

2.1 Introduction

The Menengai geothermal field has been studied since the 1960s for different objectives including geothermal resource exploration. Initial work was done by McCall (1967). He mapped the Nakuru-Thomson Falls-Lake Hannington area and the volcanoes within the Kenyan Central Rift Valley that included Menengai central volcano. In 1977, Griffith (1977) studied the Rift Valley floor and the geological formations in Menengai. Jones and Lippard (1979), Jones (1985), Griffith (1980), and Griffith and Gibson (1980) published reports on the geology of Menengai and the surrounding areas. Leat (1984) did detailed mapping, petrography and geochemical study of rocks from Menengai. He described the volcano as being entirely composed of per-alkaline and silica oversaturated rocks.

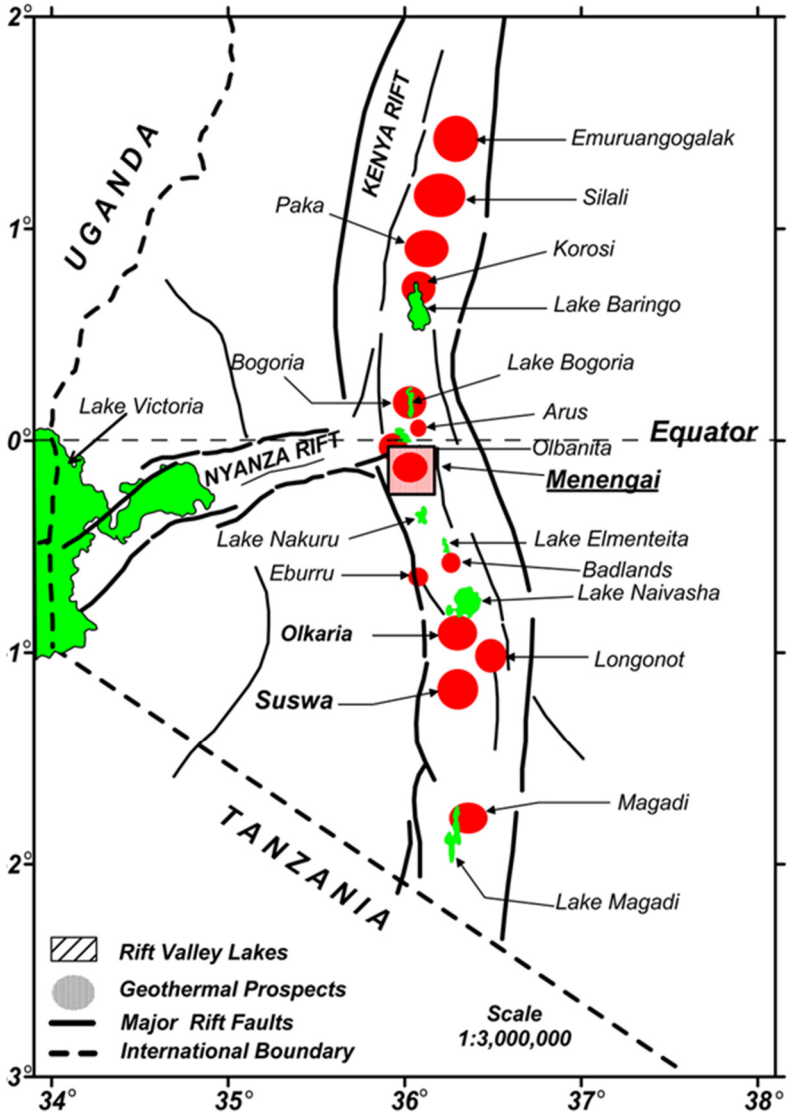

FIGURE 1: Location of the Menengai field within the Kenyan Rift Valley (Simiyu, 2009)

2.2 Geothermal exploration

Geotermica Italiana (1987) was the first group to carry out research focused solely on the assessment of the geothermal potential of Menengai. The project was coordinated and financed by UNDP and the Government of Kenya. It resulted in a detailed geological description of the area. Another detailed study was executed by KenGen (2004) covering geological, geophysical and geochemical evaluation of the prospect. The results indicated that Menengai had a potential for geothermal utilization and consequently three wells were sited. A more comprehensive study was done by the Geothermal Development Company (GDC, 2010), which resulted in a model being developed (Figure 2) that showed a great potential for resource exploitation in the area. Following the study, resistivity anomalies were identified at the Ol'rongai area, the Menengai caldera and in parts of the Solai mini graben, confirming that the resource was bigger than previously predicted and extended outside the main caldera. In addition, a geochemical soil gas survey also indicated anomalies in the above mentioned areas. Gas geothermometry suggested reservoir temperatures above 250°C. Based on these encouraging results, more wells were sited and a decision was reached to commence drilling. The Geothermal Development Company issued a drilling program from 2011 with the first well, MW-01, being successful with an average output of 5 MWe. A total of 8 wells have been drilled since.

3. SURFACE GEOLOGY AND TECTONICS

3.1 Introduction

The Menengai caldera is a trachytic central volcano underlain by a high-level magma chamber. It is one of the high-temperature fields in Kenya located within the central Rift Valley. It is presumed to be at the rift triple junction where the failed Nyanzian Rift joins the main Kenya Rift Valley that extends from Turkana in the north to Lake Natron in Northern Tanzania and is part of the East African Rift System (Figure 1). Geological units exposed at the surface can be divided into pre-caldera, syn-caldera and post-caldera volcanics. Geological mapping indicates that most of the volcanic centres, that erupted the post-caldera lavas, are located within the summit at the centre of Menengai caldera. The doming at the centre of the caldera could be a manifestation of on-going magmatic activity at depth. Therefore, it is reasonable to assume that magma is at a shallower depth around the summit. Further evidence for a near-surface magma body at the centre of the caldera is the shallow micro-seismic activity and low $\frac{V_p}{V_s}$ ratios that indicate depths of around 4-3.5 km (Simiyu, 2009). The main structures within the area are: the Ol'rongai/Molo Tectonic volcanic axis (TVA), the Solai TVA and the Menengai caldera ring faults. The Solai and the Ol'rongai TVA exhibit varying orientations, reflecting a spatial variation of tectonic stress with time.

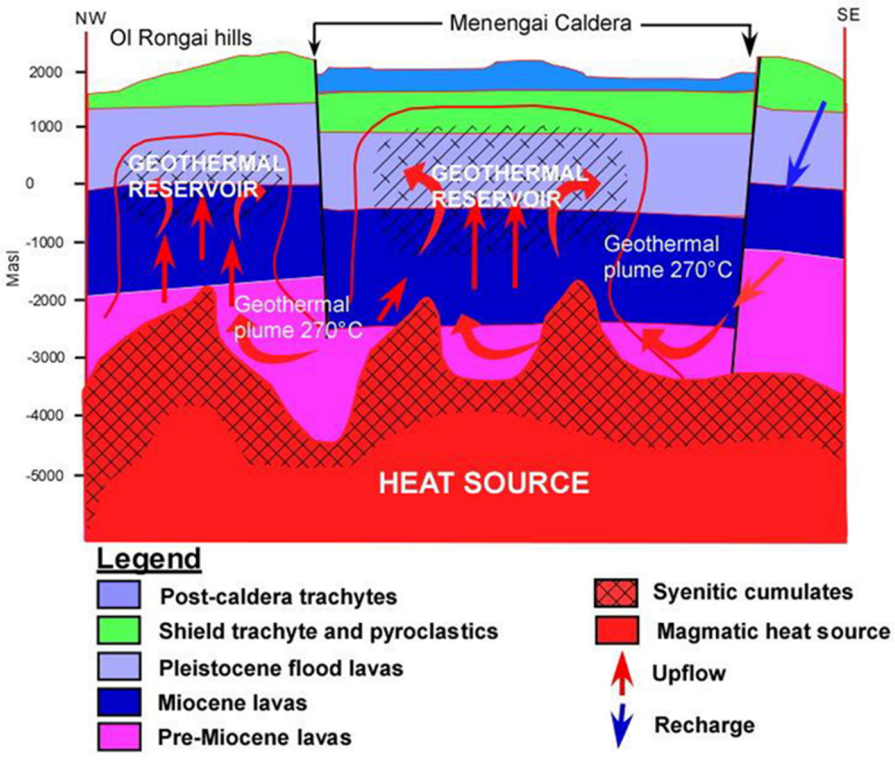

FIGURE 2: Menengai geothermal model (GDC, 2010)

3.2 Geology

The geology and evolution of the Menengai caldera is intricately tied to the volcanology of the Kenyan Central Rift Valley (see Appendix I) and is divided into three stages. These are: Pre-caldera, Syn-caldera and Post- caldera (Figure 3). The Pre-caldera stage describes a period before the caldera was formed during the Pleistocene epoch. The rocks formed during this period are not visible in the caldera floor because of the mantling by post-caldera volcanics. There are however, good exposures of these rocks at the caldera wall especially at the Lions Head cliff. The total throw of the caldera wall at the Cliff is about 300 m. The lower 235 m of the exposed deposits at the caldera wall consists of Pre-caldera volcanics (Leat 1984). The oldest outcrop is about 0.2 million years (Leat 1984) and, therefore, the shield volcano is estimated to be around this age. The shield volcanics comprise trachytic lavas with relatively uniform thickness separated by reddened soil horizons (Leat 1984) and probably with tuff or pyroclastic intercalations.

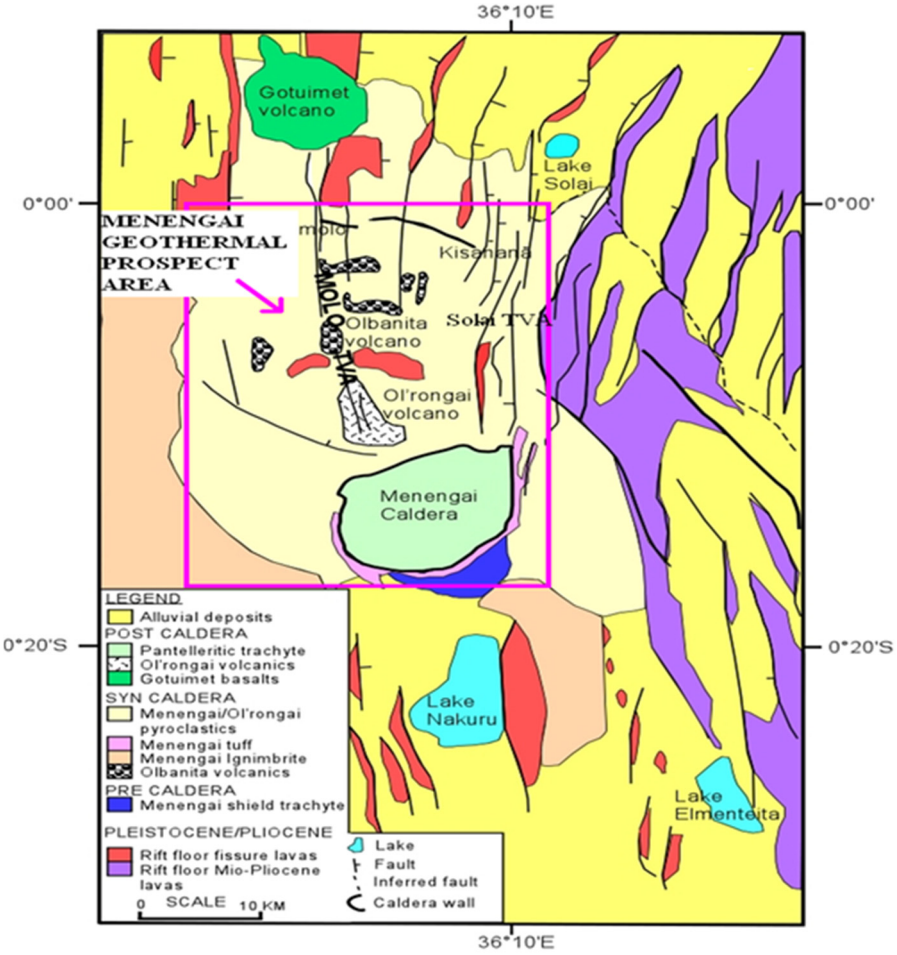

FIGURE 3: The geological map and extent of the Menengai field (GDC, 2010)

The syn-caldera stratigraphic unit is composed of a pyroclastic deposit and an ash fall deposit which is contemporaneous with the 77 km^2 (12 × 8 km) cauldron or piecemeal caldera collapse of the Menengai Volcano. This is equivalent to emptying about 30 km^3 of volatile-rich ash and pyroclastics from the magma chamber. The caldera is estimated to have formed between 12,000 and 29,000 y. BP (Leat 1984). During the post-caldera era, lava and ash eruptions continued with most of the activity being concentrated within the caldera summit. Several vents and eruption centres like "Mlima punda" can be identified within the summit area. Mlima punda is one of the cinder cones formed by an explosive eruption emit-ting scoria due to the high amounts of volatiles in the magma. Generally, all rock formations and cinder cone structures seen on the caldera floor are of the post-caldera stage. Around 25 km^3 of post-caldera volcanics were erupted, and assuming that the area of the caldera covered with the volcanics is ~80 km^2, then the thickness of the Post-caldera material will be about ~300 m. Other lithological units are the lake sediments in the northeast near the gate barrier. This formation is evidence of a paleo intra-caldera lake presumed to be from 8,000-10,000 yrs. BP as proposed by Leat (1984) and could have formed minor components of the recharge to the Menengai geothermal system. The lake was formed as a result of subterranean outflow of Lake Nakuru through structures and faults associated with the Solai system. The diatomaceous deposits associated with this Paleo-lake are overlain by post-caldera volcanics.

4. STRUCTURAL GEOLOGY

4.1 Introduction

The floor of the Menengai area (Figure 4) depicts extensional tectonics with spatial variation in the stress regime, indicated by different styles in the orientation of faults north of the caldera. The structures associated with Ol'rongai system are oriented to the NW-SE and are related to the NW-SE Menengai pre-caldera shield orientation (Leat, 1984). On the other hand, faults associated with the Solai system have a NE-SW orientation, also assumed by the Menengai caldera. Therefore, the faults appear to have

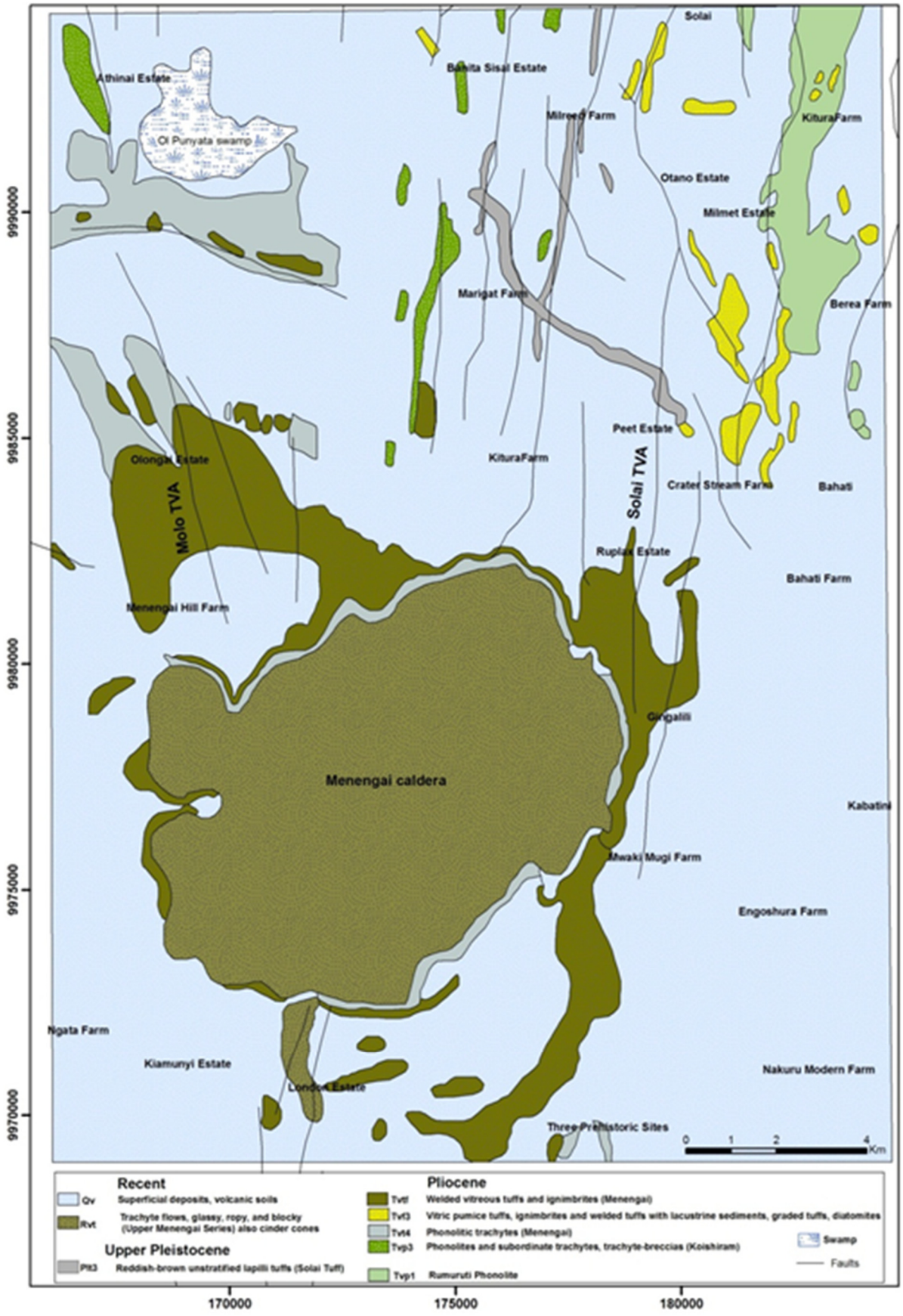

FIGURE 4: The main geological structures in the Menengai geothermal field

influenced the caldera's formation. Most structures in the Solai system can be extrapolated and cut into the caldera rim, indicating that some of these faults are in fact younger than the caldera. The variation in the orientation styles of the old NW-SE structures and the younger NE-SW structures could be due to a change or a shift in the crustal stresses. Generally, the main structures in the Menengai field (Figure 4) can be classified into 3 groups, namely:

- Ol'rongai and the Molo TVA
- The Solai structural system
- Menengai caldera and ring faults

4.2 Ol'rongai and the Molo Tectono-volcanic axis (TVA)

This structural system is represented by a concentration of faults with a NW-SE orientation. The Ol'rongai faults form part of the larger Molo TVA (Geotermica Italiana, 1987) that may have led to volcanic activities, including eruptions in the early Pleistocene epoch that resulted in an old caldera forming, referred to as the Ol'rongai volcano. The observable surface evidence of this volcano has been erased significantly, possibly by ponding of volcanic materials from Menengai volcano, erosion and sedimentation. However, gravity highs are present in this area and could represent roots or plugs that are remnants of an old magma chamber. Leat (1984) argued that the Menengai pre-caldera shield had the same orientation as the described NW-SE structures and was probably influenced by these faults. The Ol'rongai faults are, therefore, older than the ones in the Solai system which cut into the caldera. On a regional scale, the Ol'rongai system extends northwards through Lomolo and past the Gotuimet volcanic centre.

4.3 The Solai structural system

The Solai system, referred to as the Solai structural system, includes structures that extend NE-SW from the Solai area towards Lake Nakuru, south of the caldera. It comprises numerous faults/fractures, all striking in the NE-SW and NNE-SSW direction. There is a minor graben associated with these faults with its eastern boundaries extending to the foot of the Marmanent escarpment. The Solai TVA is the only system that has cut the Menengai pyroclastics at the northern end and the Pleistocene trachytes of the Lake Bogoria "Hannington" suite (Leat 1991); therefore, these faults are young compared to the Menengai caldera. The Ol'rongai and the Solai TVA seem to converge at the caldera and this has enhanced the permeability of the geothermal system in the caldera.

4.4 The Menengai caldera and ring faults

The Menengai caldera is an elliptical depression with minor and major axes measuring about 11.5 km and 7.5 km, respectively (GDC, 2010). The presence of this structure is proof of a magma chamber's existence below and, hence, a heat source. It is orientated NE-SW and appears to have been influenced by the younger NE-SW faults of the Solai system. The Solai faults formed due to a stress regime favouring a NE-SW orientation, as mentioned earlier. The caldera floor is covered with post-caldera volcanics and tectonic structures are hardly seen. Most structures striking in the NE-SW orientation can be extrapolated into the caldera, based on evidence in and around the walls: flow direction of lavas and hotspots mapped by infrared spectroscopy from the work carried out by BGR (2009) (Figure 5). At the central part of the caldera, a fissure with a NW-SE orientation has been mapped; this fissure may have resulted from transform faulting. A portion of the post-caldera lavas appears to have erupted from this fissure in a sub-plinian style (Figure 6).

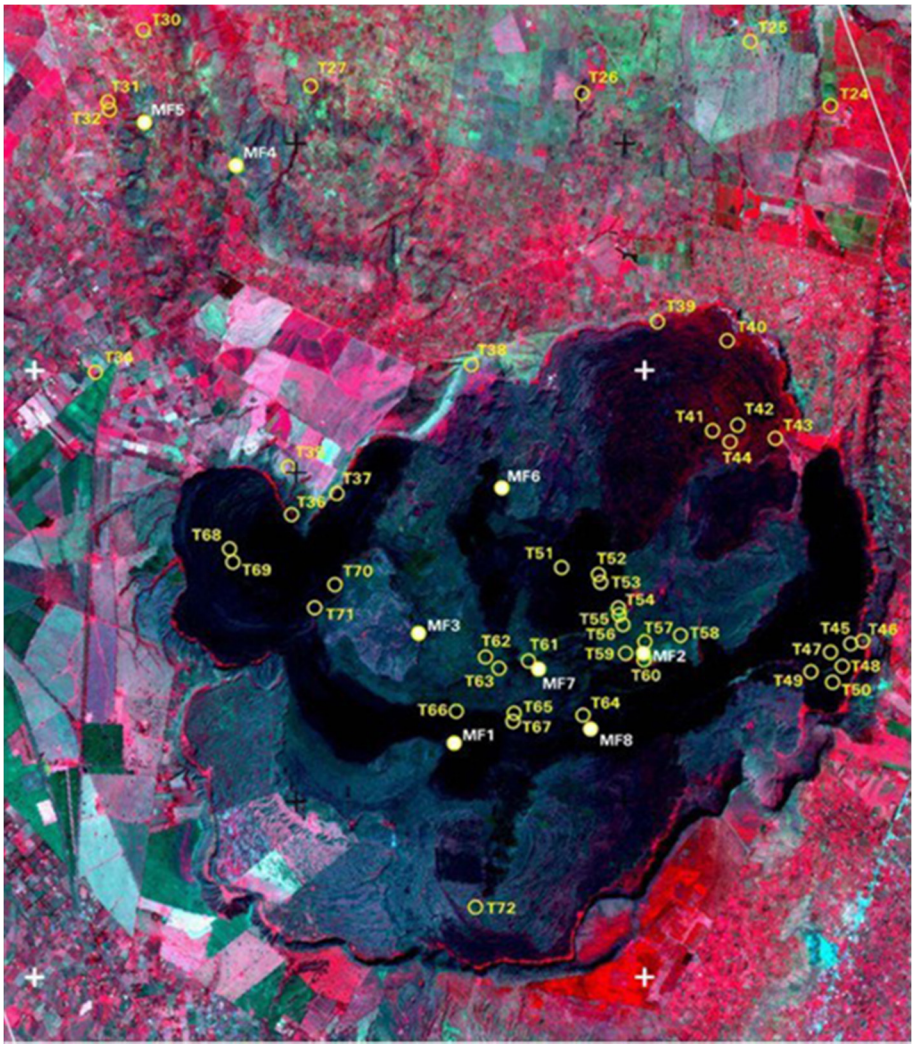

FIGURE 5: Hotspots in the Menengai geothermal field from infrared mapping (BGR, 2009)

5. SAMPLING METHODS AND ANALYSIS

Samples for this project were acquired from the Geothermal Development Company (GDC). They were sampled at a 2 m interval during drilling after which preliminary analysis was performed at the rig site through binocular microscopy. The main objective was to identify the lithology, alteration minerals, fractured surfaces and possible foreign materials in the cuttings, such as bit fragments. The aim was to develop a preliminary stratigraphy and estimate the down-hole temperatures from alteration mineralogy. This was to help in the determination of the casing depth and in advising drillers on geotechnical aspects. The samples were then processed further by washing and drying in preparation for thin-section and XRD analyses. In this project, a more detailed analysis of the samples from well MW-04 and MW-05 was carried out at the ISOR laboratories, including:

Binocular analysis: Samples were analysed at a 2 m interval using a binocular microscope. The aim was to identify lithology and alteration mineralogy. The analysis formed a basis from which samples of interest were selected for further analysis through other analytical techniques. Other features like oxidation, loss of returns, intrusions, probable aquifers and vein fillings were identified through this

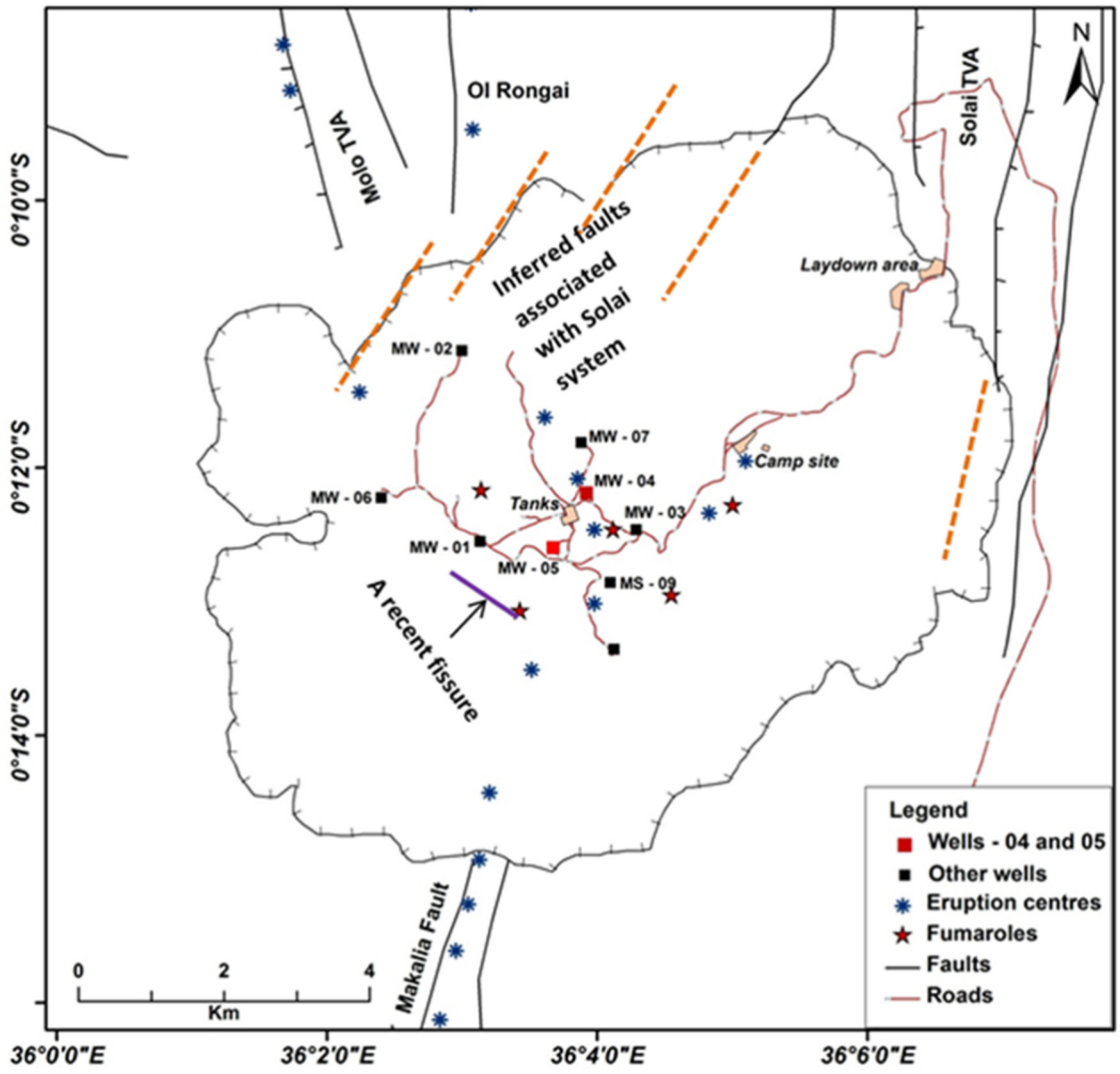

FIGURE 6: Location of wells MW-04 and MW-05

analysis. Dilute HCl was used to identify the presence of calcite; caution was taken in areas where foreign material from cement plugging or cementing of casing was suspected.

Petrographic microscopy: Thirty thin-sections from the study wells were prepared and analysed. The purpose was to identify/confirm minerals that were not exhaustively dealt with during the binocular analysis. Using this analytical method, alteration minerals like epidote, and clays were identified. The analysis made it possible for conclusive identification of the rock types and alteration minerals.

X-ray diffraction analysis: A total of 36 XRD analyses were done. Here, samples in triplets were run, i.e. untreated, glycol treated and oven-heated samples. The aim was to identify clay alteration minerals with depth and infer the temperature regime in the system.

Fluid inclusion analysis: Secondary quartz was carefully selected from a certain depth range from each well for this study. The aim was to carry out geothermometric studies to complement the alteration geothermometry. By correlating these results with the measured temperatures, the dynamics of the geothermal system through time was outlined. Finally, all data sets were integrated using Log-Plot software (RockWare, 2007) for interpretation, data management and storage for easy retrieval.

6. BOREHOLE GEOLOGY

6.1 Drilling at Menengai

Exploration drilling in Menengai kicked off in February of 2011 after comprehensive geoscientific studies, which culminated in a conceptual model being developed. A total of 8 wells are located within the Menengai caldera. Wells MW-04 and MW-05, highlighted in Figure 6, are among these. The two wells were aimed at tapping the NE-SW generally trending faults and the NNW-SSE structures associated with the Molo TVA. The purpose of the wells was to further explore the field in order to determine: the availability of the resource, the depth and temperature of the reservoir and chemical characteristics of the reservoir fluids.

6.1.1 Drilling of well MW-04

The well was spudded on 18 July 2011 and was completed on 8 Oct 2011 after 81 days (Figure 7). The surface 26“ hole was drilled to a depth of 81.87 m with intermittent losses experienced. The 20“ surface casing was set at 80.87 m where primary and secondary cementing was done. Three backfill cement jobs were done in this section with a total of 20.33 tons of neat cement being used to bond the 20“ 94 PPF BT casing. The 17½” hole was drilled to a depth of 403.2 m after which anchor casing was set at around 401.2 m. A mass of 29.19 tons of blended cement and 40.5 tons of neat cement were used in bonding the 13⅜“ 54.5 PPF BT casings at this section. The 12¼“ hole was drilled to a depth of 1,106 m where 9⅝“ 47 PPF BT production casings were set. This section of the hole was drilled with aerated water and foam, thus achieving continuous circulation with minimal intermittent losses. A total of 34.54 tons of blended cement and 52.15 tons of neat cement were used for cementing the production casings.

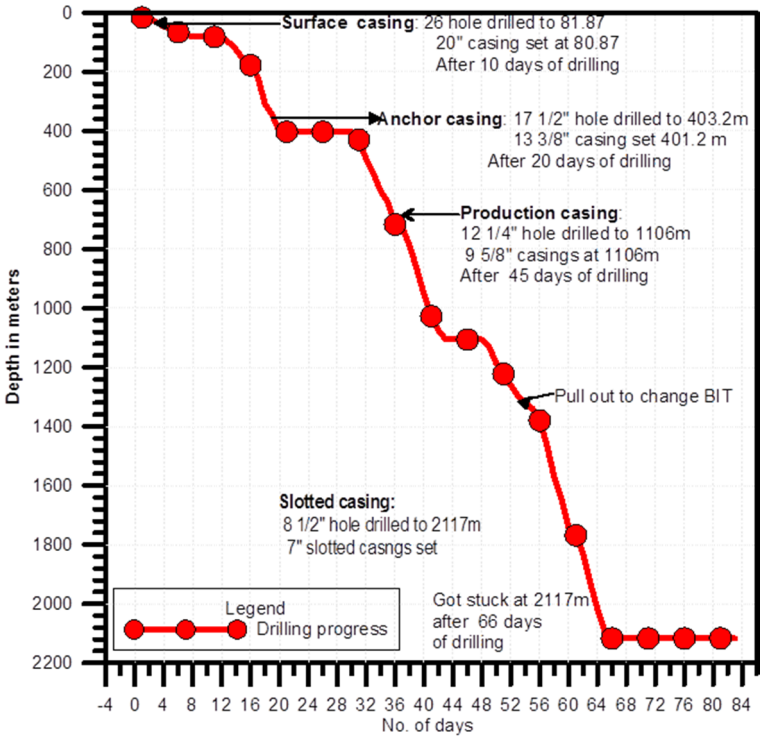

FIGURE 7: Drilling progress of well MW-04

The 8½“ hole was drilled to a depth of 2,117 m after which the drill string got stuck. After several attempts to free the string, success was attained. On pulling out, a part of the string consisting of the bit, the bit sub, the cross-over sub, the stabilizer and 2 drill collars were left in the hole. The total length of the BHA lost was about 20.4 m. Thus, the maximum clear depth of MW-04 is 2,096.6 m RKB. At the end, a 7“ 26 PPF BT slotted liner were run into the hole and set above the fish.

6.1.2 Drilling of MW-05

The well was spudded on 26 October 2011 at 00:50 hours and was completed on 29 January 2012 at 10:00 hours, after which the rig was released for demobilization. The drilling progress is highlighted in Figure 8. The surface hole was drilled using the 26“ bit to a depth of 81.0 m RKB, using mud and water as the drilling fluids. The 20“ surface casing was set at 80.0 m, totalling about seven joints in the hole.

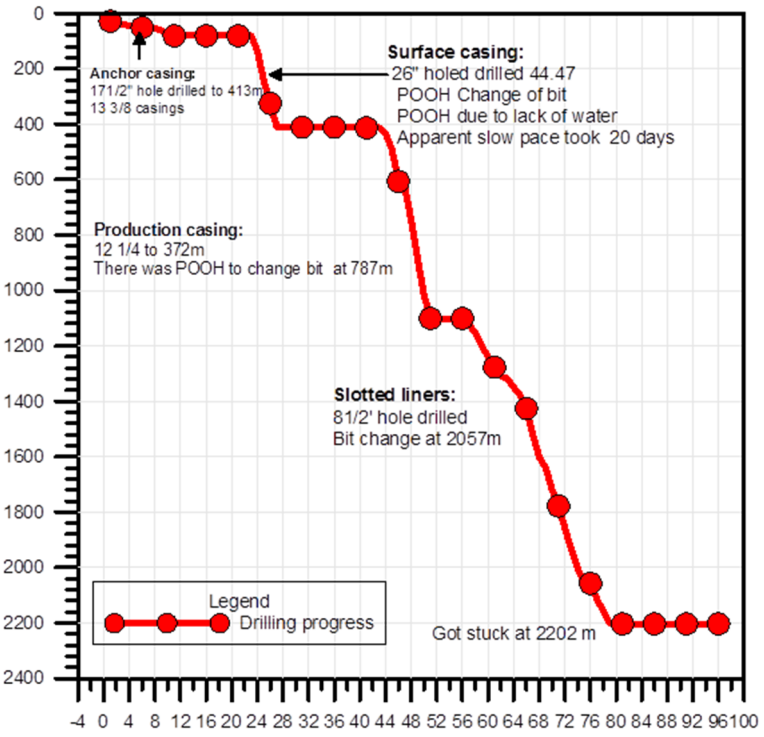

FIGURE 1: Drilling progress of well MW-05

Cementing operations followed with a primary cement job and three backfills with 35.06 tons of cement being used. The intermediate hole was drilled with a 17½“ bit to a depth of 413.0 m with the 13⅜“ casing being set at a depth of 409.0 m RKB. A total of thirty seven 54.5 lb/ft and two 68 lb/ft joints were run in the hole. A mass of 124.49 tons of cement was used for both the casing and plugging jobs.

The production hole was drilled with a 12¼“ bit to a depth of 1,101.09 m. The main drilling fluids in this section were aerated water and foam. Some losses were encountered, especially at 1,025-1,032 m. The 9⅝“ casing was set at a depth of 1,100.59 m RKB with a total of 98 joints. A mass of 90.44 tons of cement was used in this section for both the casing and plug jobs. Full cement returns were observed on the surface after five backfills. The main hole was drilled to a depth of 2,202.96 m, using an 8½“ bit for the entire section; aerated water and foam were used as the drilling fluids. Sweeps with high viscosity mud were employed after every 5 m to ensure thorough removal of cuttings. The drill string got stuck at a depth of 2,202.96 m. Several attempts were made to free the string with over-pulls ranging from 133 kN-244 kN. The string was freed on 24 January 2012 at 07:00 hours On POOH to inspect the string, the 8½“ bit, the bit sub and 2 drill collars were left down hole. The length of BHA left in the hole was 21.21 m, thus the maximum clear depth of MW-05 was 2,181.69 m RKB. A total of 97 joints of 7“ 26 PPF BT slotted liners and 2 plain joints were run into the hole.

From the editor: The name of the well “MW-05” needs explanations. When drilled this well was named MW-06, but was later officially renamed as MW-05 by GDC, and that name is used here. In early 2013 the well was again renamed, and got back its old number, MW-06.

6.2 Stratigraphy

The description of the lithostratigraphy is mainly based on the binocular stereo microscope observations aided with petrographic analysis of thin-sections. Menengai is predominately trachytic, however layers of tuffs and pyroclastics are encountered. The trachytes have been classified into three classes, based on their grain sizes. On a regional scale, the rocks can be described as being pre-caldera, syn-caldera and post-caldera volcanics. Pre-caldera rock units are encountered below 400 m and are associated with the Menengai shield lavas, Ol‘rongai volcanics and probably Lake Hannington trachytes (Appendix I). The syn-caldera rock comprise a greenish brown to brown tuff layer between 320 - 400 m, resulting from a voluminous ash eruption just before the caldera collapsed during the late Pleistocene epoch. On the other hand, post-caldera is associated with Holocene lava eruptions and pyroclastics from vents and cone structures within the caldera floor. Figure 9 is an evolution model of the Menengai caldera in relation to the pre-caldera, syn-caldera and post-caldera stratigraphic units described above. A detailed description of lithological units in Menengai caldera, based on results from wells MW-04 and MW-05, is given below.

Pyroclastics are loose unconsolidated extrusive rocks. They form the uppermost 5-20 m. They are also conspicuous as thin lenses in the upper 300 m of the stratigraphy, signifying several pyroclastic eruptions in the post-caldera stage. The source of these pyroclastics is the cone structures, e.g. Mlima Punda that formed after the caldera collapse. The pyroclastics are brownish grey to brown, fine grained and vesicular scoria and pumice with sanidine phenocrysts. The rock shows no alteration in the upper 20 m but is oxidized. At depth, alteration is evident with vesicles being filled with zeolites and clays.

Tuffs are encountered in several parts of the wells but significant layers are intercepted at 300, 700 and at 1,500 m. The layer between 300-400 m is presumed to be a marker horizon, separating the pre-caldera and the post-caldera volcanic stages. The marker unit is thin in well MW-05 when compared with well MW-04. Generally, the tuffs can be classified into three groups which are: lithic tuff, welded tuff and vitric tuff. The lithic and vitric tuff are light grey in colour, poorly crystalline and massive to vesicular rocks, while the welded tuff is dark grey and fairly crystalline.

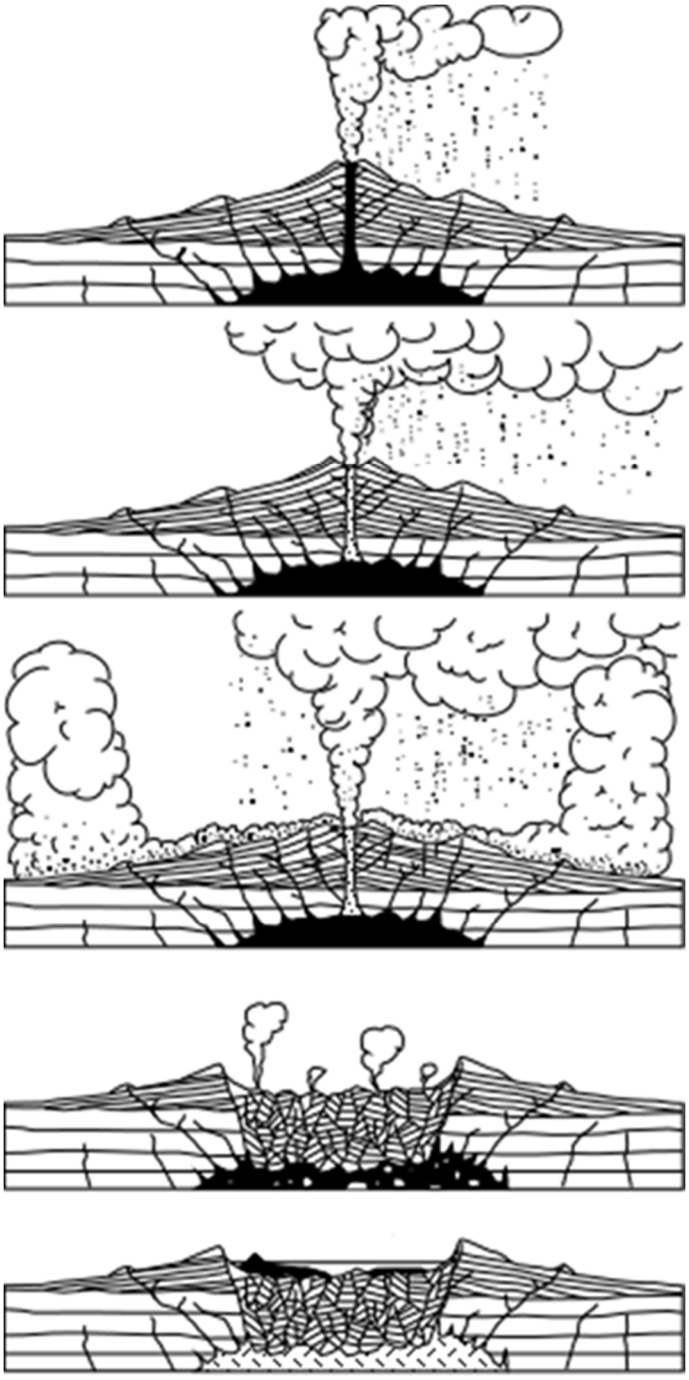

FIGURE 9: Caldera evolution (Nelson, 2011), comparable to the Menengai evolution

Trachytes are the dominating rock units in Menengai. They are highly fractured and blocky at the upper 50-80 m and present drilling challenges with persistent circulation losses being experienced at this zone. In an effort to differentiate episodes of lava eruptions, trachyte is classified into three groups based on its grain sizes; these are: fine-grained, medium-grained and coarse-grained trachytes. Although the chemistry of these rocks may vary slightly, textural classification is preferred, considering that the main analysis in this project was through binocular stereo microscopy. Menengai trachytes generally range from grey, brownish grey to light grey in colour. They are strongly porphyritic with large conspicuous phenocrysts of sanidine feldspars set in a feldspar groundmass with trachytic texture. The sanidine is well formed showing good crystal outlines appearing somehow as elongated rectangles and nearly always showing simple twining. The rock is altered to variable degrees at different depths with main mafic minerals being pyroxenes and amphiboles; however, magnetite and titano-magnetites are noted under petrographic analysis.

Intrusions. Menengai caldera is hosted in a spreading zone, hence, fresh magma pulses from the main magma chamber are readily injected into the overlying formations, forming dikes and other intrusions.

These magma injections are facilitated by faults and fractures resulting from the tectonics associated with a divergent plate setting. Evidence of intrusions has been identified in the stratigraphic column of the two wells. In well MW-05, such intrusions are encountered at 264, 424, 606, 1,150, 1,678, and 2,084 m and at the bottom of the well where fresh glass was intercepted. In well MW-04, intrusions were encountered at 490, 1,458, 1,956 and 2,082 m. Generally, the intrusions are fresh, coarse- to medium-grained and, in some instances, specifically at 2,082 and 2,172 m in wells MW-04 and MW-05, respectively, it is a fresh chilled glass. The coarse-grained type units are intercepted at shallow depths (200-400); they are grey, phyric with feldspar and pyroxene phenocrysts. The medium-grained intrusion has unique prismatic dark minerals suspected to be amphiboles with a feldspathic groundmass; they are intercepted at 1,956 and 400 m in wells MW-04 and MW-05, respectively.

Chilled fresh glass was encountered at 2,082 and 2,174 m in wells MW-04 and MW-05, respectively, indicating a possible intrusion of magma. This is because glass is susceptible to alteration and at such depths in high temperature geothermal system such as Menengai; it would have altered completely unless it was a very recent intrusion that was chilled by the drilling fluid. Drilling challenges were experienced at these depths, i.e. sticking of the drill string and anomalously high temperatures were recorded at the bottom of these wells. This is probably due to a high heat flow influx from the magmatic intrusion into the country rocks. The characteristics of the fresh glass under a binocular microscope include stretched vesicles. In thin-section, the stretched vesicles are more pronounced, forming a typical characteristic of highly volatile magma. Sieved texture in sanidines was identified in thin section, possibly reflecting a rapid decompression due to quick ascent of the magma through cracks into the overlying formation. Further discussion on this is constrained until the results on the proposed analysis on the volatiles components of the glass, microprobe data and short lived isotope analysis are available.

Reddened soils (red-beds). Eruption episodes in the pre-caldera period were discontinuous and, sometimes, long periods of time passed before an eruption was experienced; this allowed soils to form and even windblown sediments to be deposited. A later eruption issuing lava would flow over the soils and, in the process, bake them, turning the appearance into an anomalous red colour. Leat (1984) observed these type of reddened soils separating lava sequences at the Lions Cliff where pre-caldera lavas are well exposed. It is, therefore, presumed that we would drill through into these soils, especially below 400 m where the Pre-caldera lavas are encountered. The reddish sample cuttings, e.g. between 1,614 and 1,638 m in well MW-05, and the reddish outflow experienced occasionally during drilling, could be pointers to the presence of the described soils. Red beds are also encountered in the Tertiary lava sequence in Iceland and have often led to drilling difficulties. When they are in contact with drilling fluids, they disintegrate rapidly, leading to huge cavities forming in a drill hole. These cavities make it hard for effective circulation and transportation of cuttings to the surface. The cuttings pile up in these cavities and eventually fall back into the drill hole, choking the drill string and causing it to get stuck.

6.3 Stratigraphic correlations

A geological cross-section across wells MW-04 and MW-05 is highlighted in Figure 10. The figure reveals in detail the subsurface geology in the area around the caldera summit. Four tuff marker horizons were identified. The upper 300 m is composed of Holocene post-caldera lavas, tuffs and pyroclastics. The youngest lavas are easily seen on the surface, due to their pristine nature, and are around 1,400 years old (Leat 1984). These post-caldera lavas make it hard to decipher geological structures on the caldera floor by simple observations, so other techniques in exploration geology like magnetics or gravity would probably be more helpful in mapping these structures. The syn-caldera formation is a greenish brown to brownish tuff layer at 320-400 m depth. It is related to tuff marker horizon 1 and separates the post caldera from the pre-caldera sequences. Literature review indicates that it is between 29,000-12,500 years (Leat, 1991). The pre-caldera forms the biggest part of the stratigraphic column and is marked by tuff layers at 700 m (horizon 2), 1,600 m (horizon 3) and 1,800 m (horizon 4). There is a massive lava sequence from 1,200 to 1,400 m that appears very competent and not altered at all and could also be a marker horizon in the pre-caldera sequence. The loss of returns experienced at the pre-caldera sequence

is mostly due to unconformities at the rock contacts or faults between lavas and tuff layers forming feed zones.

6.4 Hydrothermal alteration and fluid chemistry in Menengai

Rock alteration simply means changing the mineralogy of the rock. The primary minerals are replaced by the secondary minerals because there has been a change in the prevailing physiochemical conditions subjected to the rock. This could be changes in temperature, pressure, or chemical conditions. Henley and Ellis (1983) described hydrothermal alteration as a general term embracing change in mineralogy, texture and chemistry of rocks due to thermal and environmental changes facilitated by geothermal fluids and gases. The intensity of the changes would not only depend on temperatures but also on texture and time. Reyes (2000) suggested that hydrothermal alteration is affected by temperature, permeability, fluid composition and rock composition. Hydrothermal alteration is, therefore, a thermodynamic process affecting unstable minerals at certain conditions.

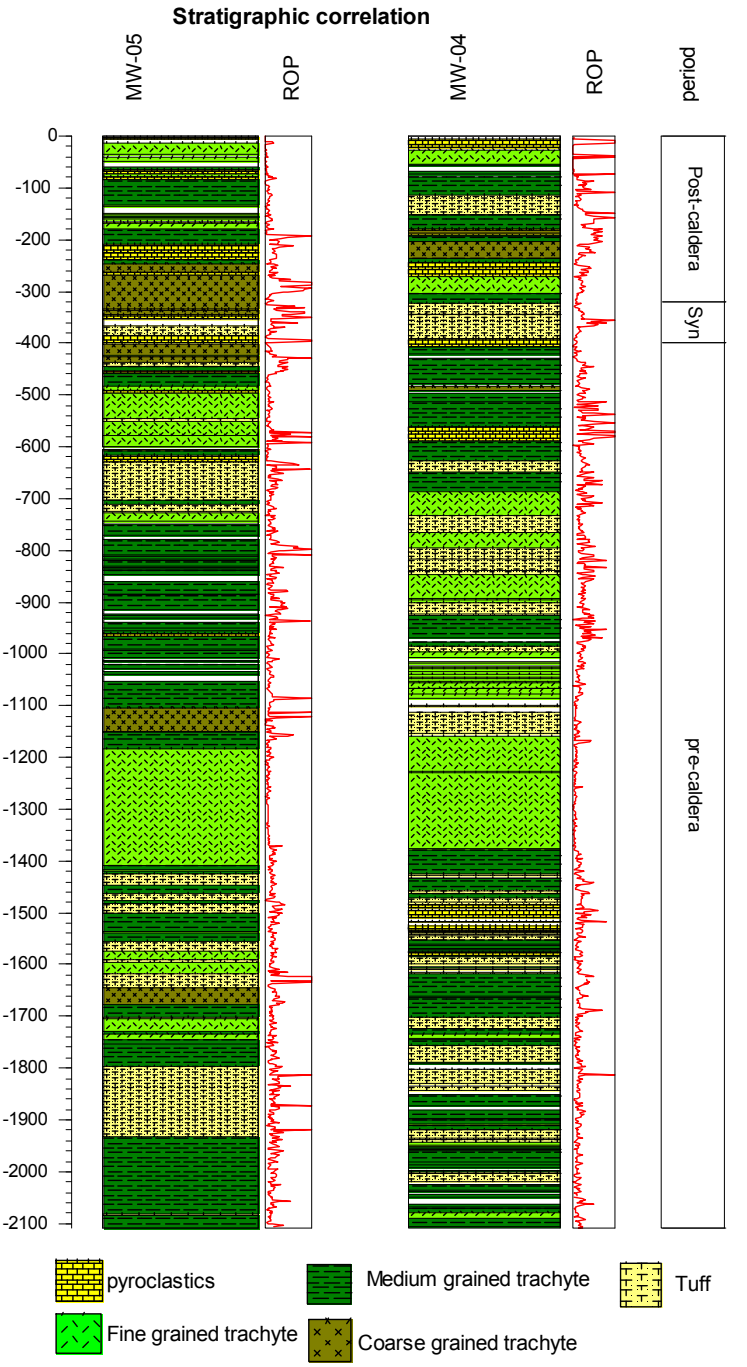

FIGURE 10: Stratigraphy and stratigraphic correlation between wells MW-04 and MW-05

Generally, in geothermal systems like Menengai, secondary minerals form as a result of the interaction of the rock with hot water fluids, known as hydrothermal fluids. The fluids carry metals in solution, either from a nearby igneous source or from leaching out of nearby rocks. They may contain various types of gases, salts (briny fluids) and metals and, therefore, fluid composition is extremely variable (Lagat, 2008). Hydrothermal fluids cause alteration by interacting with reservoir rocks, changing their composition by adding or removing or redistributing chemical components. Temperatures can range from ambient to boiling. There are two main possible sources of hydrothermal fluids, a) meteoric water, which is possibly the main source of hydrothermal fluids; and b) juvenile water from a magmatic source, but this is commonly a minor component.

The number of hydrothermal alteration minerals in Menengai is not only constrained by the rock composition but also by fluid chemistry. Previous studies on fluid geochemistry from well MW-01 data

by (Kipng'ok, 2011) indicated that Menengai water could be of Na-HCO_3 type with high Cl and CO_2 contents, assuming that the chemistry is invariable. Calculation of saturation indices (SI) to estimate hydrothermal alteration mineral equilibrium with fluids in wells MW-04 and MW-05 was constrained by the lack of sufficient data. The SI calculation would have been a good estimation of alteration minerals in equilibria with the system in the two wells. However, application of these calculations may not be very straightforward (Karingithi et al., 2010). A general model of hydrothermal mineral alteration in Menengai is highlighted in Figure 11.

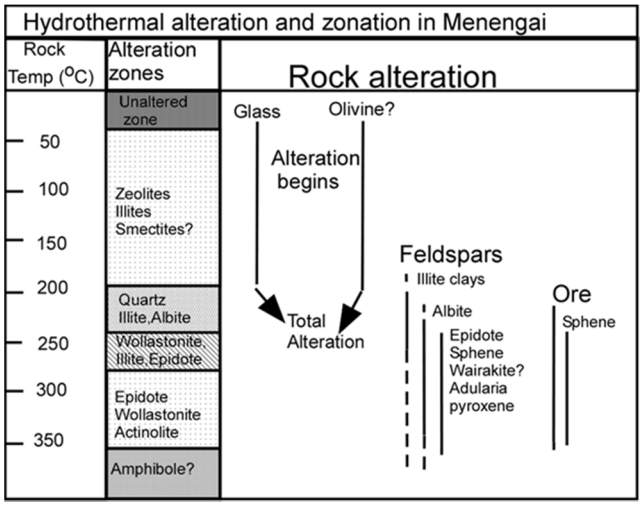

FIGURE 11: Hydrothermal alteration and temperature variation (modified from Franzson, 1998)

6.5 Distribution of hydrothermal alteration minerals in wells MW-04 and MW-05

The main hydrothermal alteration minerals in wells MW-04 and MW-05 are described below (see Appendix II for the chemical formulae). The distribution of the main minerals in MW-04 and MW-05 are further presented in Figures 12 and 13.

Zeolites are first observed at 244 m in well MW-04 and 178 m in MW-05. The types found are cowlescite and the radiating scolecite/mesolite. They occur as vesicle infillings, mostly in the pyroclastic layers. Zeolites are generally thermodynamically metastable at ~<110 °C. The interval between 178 and 500 m forms the zeolite zone.

Pyrite is a cubic mineral with a metallic lustre and sometimes the yellowish gold colour is more pronounced. It is disseminated in the groundmass of feldspars. It is encountered almost throughout the well depth but it is most abundant between 1,000 and 1,500 m in the two wells. It is an indicator for permeability whereby interaction between the geothermal fluids rich in H_2S has been on-going for a period of time.

*Pyrrhotite***.** It is not a very common alteration mineral in the Menengai wells. It was, however, identified in well MW-05 at around 550 m. It has a brownish colour and is a form of an iron sulphide mineral.

Albite occurs as an alteration mineral from feldspars. Albite alteration occurs at around 500 m but extensive albitization is seen at 750 m in both wells. Below 1,900 m, clear euhedral albite crystals were identified.

Chalcedony is first encountered at 172 and 186 m in wells MW-05 and MW-04, respectively. It is also encountered at 310, 348 and 488 m in well MW-05. It is milky white and extremely fine grained and massive. It begins to be replaced by quartz at 856 and 500 m in wells MW-04 and MW-05, respectively.

Clays. XRD analysis was done on 36 samples from selected depths in the two wells (Appendices III and IV). The results indicate that there is a very small amount of clays in Menengai. Illite clays were present mainly from 900 to 1,900 m in both wells, while smectites were present between 190 and 350 m and at a deeper zone between 600 and 1,100 m. The smectites at deeper depths could be relict.

Calcite occurs as dissemination in the groundmass and can be detected by the use of hydrochloric acid (HCl) in the initial analysis. It occurs intermittently throughout the wells but disappears after 2,050 m in both wells. Platy calcite was identified at 1,238 and 1,534 m in well MW-05 and could signify boiling

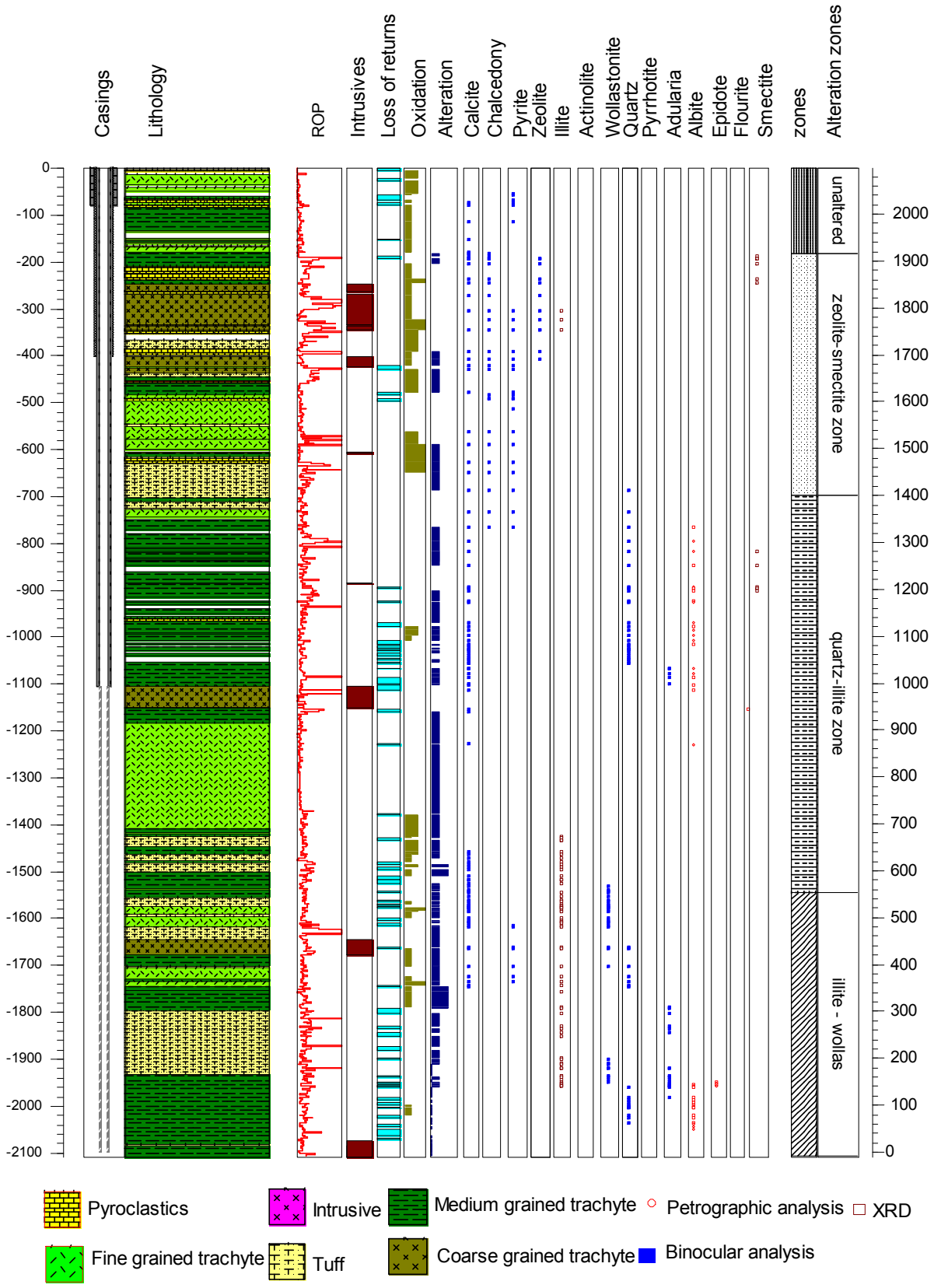

FIGURE 12: Hydrothermal alteration mineral distribution of well MW-04

in these zones (Thompson and Thompson, 1996). It is abundant at 1,300-1,500 m in well MW-05 and at 1,578 m in MW-04, as noted in both binocular and thin sections analysis.

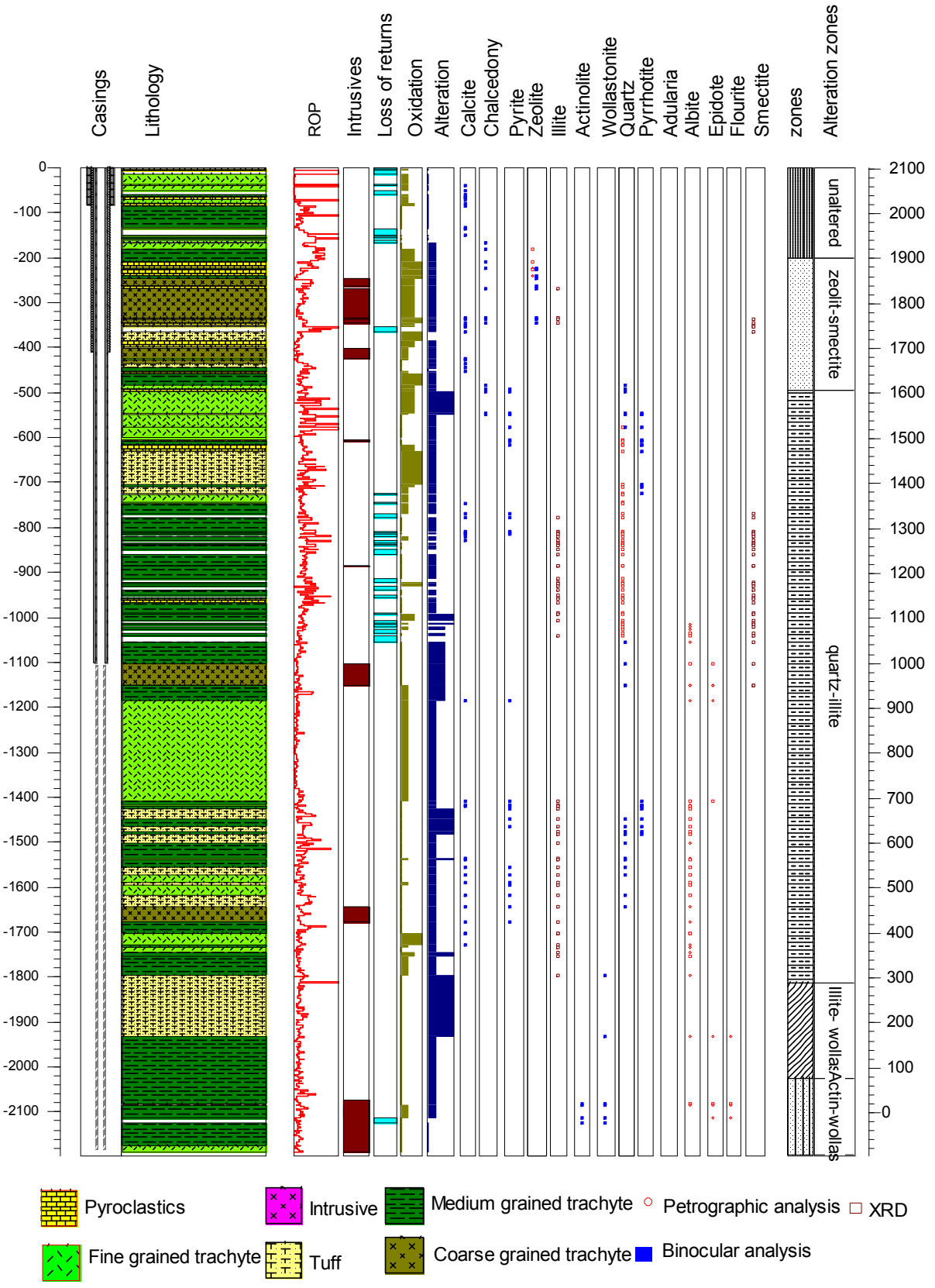

FIGURE 13: Hydrothermal alteration mineral distribution of well MW-05

Quartz. Secondary quartz was found below 580 m and persists almost to the bottom of both wells. At shallow depths, it was identified as a replacement to chalcedony while at deeper depths they deposited in vugs. Quartz is a hexagonal mineral, stable in geothermal systems above 180°C.

Epidote. Analysis of cuttings indicated that epidote is actually rare in the two wells. Epidote occurrence is evident at 1,956 m in well MW-04 and at 1,100, 1,460 and 1,970 m in well MW-05, based on thin section analysis. Calculation of mineral saturation indices from well MW-01 data indicates that epidote is under-saturated (Kipng'ok, 2011). This fact, coupled with high CO_2 concentrations, probably makes epidote an unstable mineral in Menengai, assuming that conditions are the same in well MW-01, MW-04 and MW-05 and that epidote can disintegrate easily. Epidote could also be rare in Menengai because it is a young geothermal system and the mineral has not had time to form.

Wollastonite is an alteration mineral often associated with contact metamorphism and, therefore, its occurrence is probably related to the numerous intrusions in the caldera summit area. It occurs at 1,544 and 1,824 m in wells MW-04 and MW-05, respectively. It is colourless and fibrous under the binocular microscope and indicates temperatures of ≥270°C.

Actinolite. This is an alteration mineral classified in the asbestos (amphibole) mineral group. It is a high-temperature mineral, forming greenish radiating, acicular crystals or massive to granular aggregates in the groundmass. It is formed by the replacement of ferromagnesian minerals. Actinolite appeared at 2,024 m in well MW-05 but was not present in well MW-04. It indicates temperatures of above 280°C.

6.6 Geothermometry

6.6.1 Alteration mineral geothermometry

Hydrothermal alteration minerals are stable at certain temperatures and pressures. However, in geothermal systems, pressures are not considered a key parameter. It is on this assumption, therefore, that alteration minerals are used as geothermometers. Figure 14 is a calibrated geothermometric scale for various minerals based on studies by Reyes (2000). This scale has been applied in hydrothermal alteration mineral geothermometry in Menengai. The inferred reservoir temperature is between 200 and 270°C which is based on the occurrence of quartz, illite and wollastonite at the upper levels of the reservoir. The lower part of the reservoir is estimated to be at a temperature >270°C, based on the occurrence of wollastonite and actinolite.

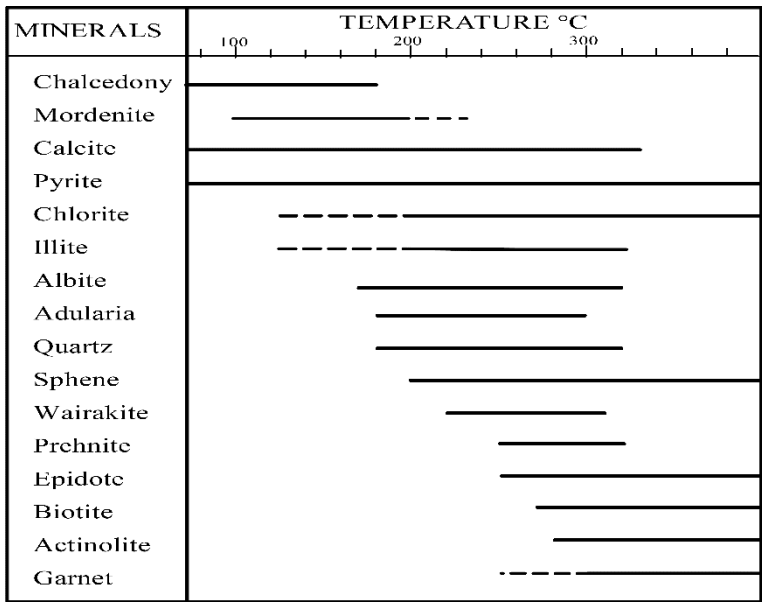

FIGURE 14: Mineral geothermometry (Reyes, 2000)

6.6.2 Fluid inclusion geothermometry

Fluid inclusion homogenization temperature gives the minimum temperature of entrapment of a fluid in a mineral. Fluid inclusions trapped in quartz at 1,500 m from each well were analysed. This zone forms

part of the upper reservoir zone, estimated to be between 200 and 280°C, based on hydrothermal alteration minerals. All inclusions were classified as either primary or secondary. Primary inclusions were trapped at the time of mineral growth, whereas secondary inclusions were trapped along healed fractures. Heating was done on handpicked crystals using a Linkam THSMG 94 freezing and heating stage. Temperature results from well MW-04 ranged from 180 to 240°C with an average value of 240°C. The low temperature values of 180-185°C are assumed to be from secondary inclusions because they are much lower than the average values. Well MW-05 has a temperature range between 200 and 258°C, with an average value of above 245°C. The homogenisation measurements were recorded at 5°C intervals.

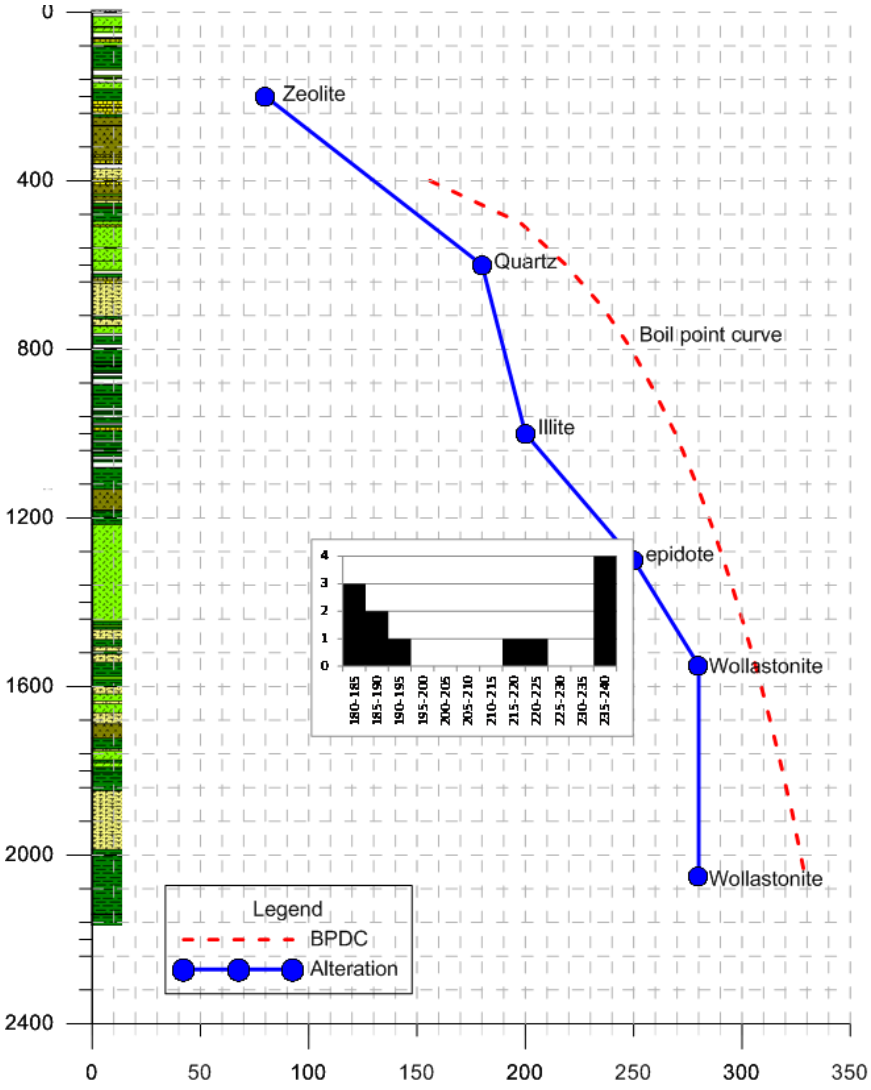

FIGURE 15: Measured, alteration and fluid inclusion temperature profile of well MW-04

These results reveal slightly lower temperatures compared to the alteration mineral temperatures and measured temperatures; therefore, the system is probably heating up. Correlations between fluid inclusions, alteration minerals and measured temperatures are highlighted in Figures 15 and 16.

6.7 Mineral zonation

Based on this study, four hydrothermal alteration zones were identified, as highlighted in Figure 17. At shallow depths, the rocks are unaltered and remain reasonably fresh but oxidized. The zeolites-smectite zone is the uppermost zone and is characterized by the occurrence of various zeolites and minor smectite. The zeolite index minerals were mainly cowlescite and mesolite/scolecite. The second zone that forms the upper part of the reservoir is the illite-quartz zone. It is marked by the occurrence of quartz as a replacement for chalcedony and illite clays. However, a portion of this zone i.e. 1,200-1,400 m, shows no alteration and is characterized by massive relatively fresh lava. The middle part of the reservoir is the illite-quartz-wollastonite zone, characterized by the illite, quartz and wollastonite encountered at 1,544 m in well MW-04 and at 1,812 m in well MW-05. The final zone, which is a deeper reservoir zone, is the wollastonite-actinolite zone. It is well defined in well MW-05, but inferred in well MW-04 because actinolite was not present.

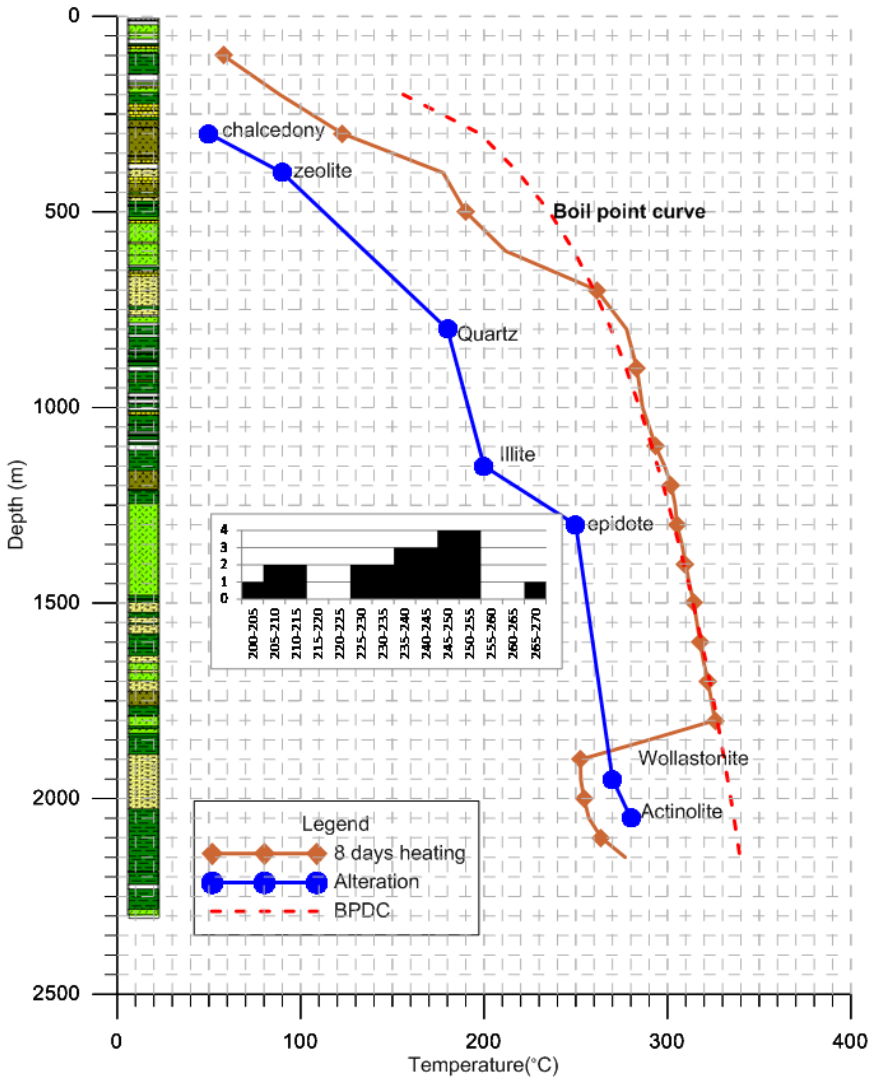

FIGURE 16: Measured, alteration and fluid inclusion temperature profile of well MW-05

7. PERMEABLE ZONES

The main objective in geothermal drilling is to intersect high-temperature permeable zones. Such permeable zones, related to either faulting, jointing, intrusions and lithological contacts, are termed feed zones/aquifers. Shallow aquifers and feed zones are cased off and cemented, to prevent the shallow cold water from cooling as well, and also for safety reasons. Permeable zones in a well can be identified in several ways such as: the use of circulation losses (Koestono, 2007), the use of temperature logs (Danielson, 2010), the hydrothermal alteration minerals that are present, and by the degree of hydrothermal alteration and lithological conditions. Caution should be taken, however, when using losses as way of identifying an aquifer, since losses can be caused by many other drilling factors, especially when employing aerated drilling, as in Menengai. In Menengai, all loss zones less than 2 m were eliminated, as these are minor losses that could have occurred when adding a drill pipe etc. and cannot, therefore, be termed real loss zones. Temperature peaks in profiles measured during drilling, and breaks in the temperature increase seen during the heating up period, suggest permeability. According to Lagat (1995), the use of temperature logs may have an error of up to 10 m. Reyes (2000) suggested that alteration minerals like quartz, abundant calcite, abundant pyrite, anhydrite, wairakite and illite are good indicators of permeability. On the other hand, minerals like prehnite, titanite,

persistent smectite and pumpellyite are indications of poor permeability. In wells MW-04 and MW-05, several permeable zones were identified and are highlighted in Figures 18 and 19. These are based on the many factors discussed above, including the penetration rates.

7.1 Well MW-04

Well MW-04 is a very permeable well, based on the significant circulation losses experienced (Figure 18). At shallow depths, i.e. 0-200 m, the losses experienced were due to a highly fractured blocky trachyte. At 200-500 m, there are intermittent losses in the well correlating with high penetration rates. Alteration at this zone is low but the rocks are highly oxidized, probably due to the effects of shallow underground water or because of closely spaced contact zones due to the thin post-caldera lavas. Geothermal aquifers were observed at varying depths from 850 m to the bottom of the well. There identifications were based on circulation losses, lithological characteristics and measured temperatures. Five aquifers were mapped, namely:

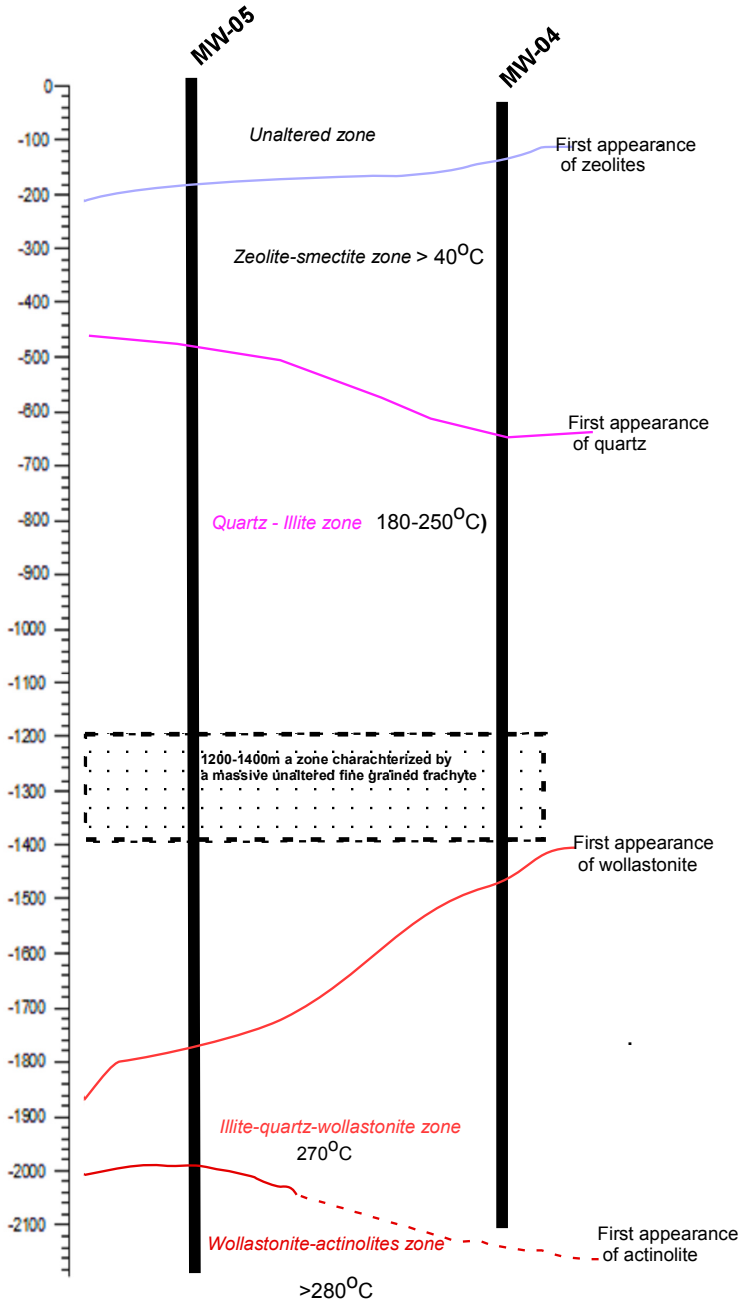

FIGURE 17: Hydrothermal zonation

Aquifer 1 is located at 850 m and is related to a medium-grained trachyte. Loss of circulation, high penetration rates and the peaks in the measured temperatures were considered when mapping this aquifer.

Aquifer 2 is located at 900 m and is also related to a medium-grained trachyte. There is a relatively sharp increase in the measured temperature, indicating that the aquifer could be slightly bigger than the one at 850 m.

Aquifer 3 is at 1,050 m; it is similar to the first two aquifers mentioned. Aquifers 1, 2 and 3 were all cased off.

Aquifer 4 is a zone between 1,400 and 1,500 m where lenses of tuffs and a medium-grained trachyte are encountered. It is a very permeable zone, based on the losses experienced. The measured temperature shows a higher peak, indicating that this could be the main aquifer in the well.

Aquifer 5 is at 1,950 m and is probably related to a contact between a tuff and medium-grained trachyte. Measured temperatures appear here compared to the relatively colder tuff region above.

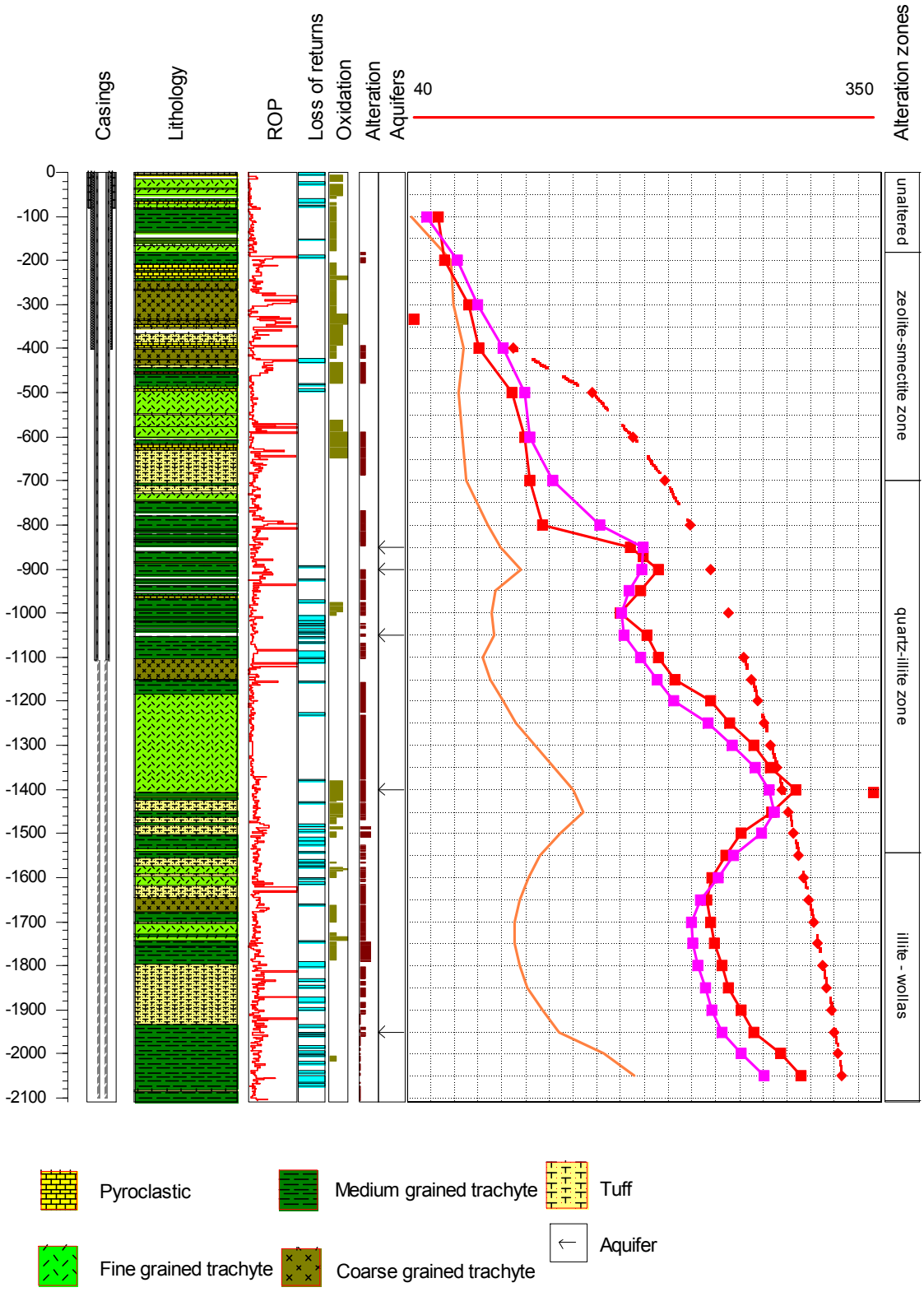

FIGURE 18: Permeable zones in well MW-04

7.2 Well MW-05

Well MW-05 appears to be less permeable than well MW-04, based on the circulation losses experienced (Figure 19). This well has similar losses as well MW-04 at shallow depths, related to the

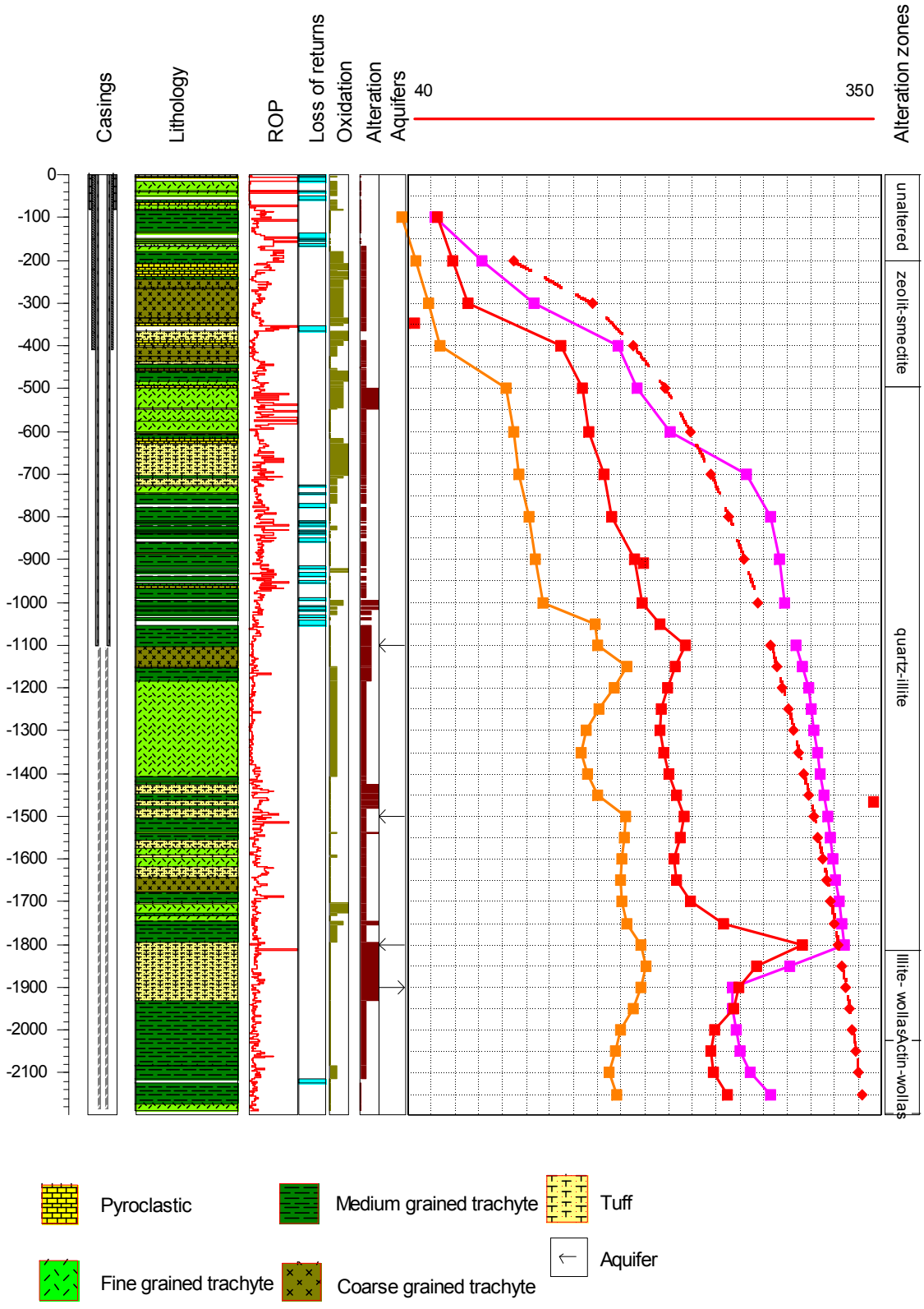

FIGURE 19: Permeable zones in well MW-05

fractured blocky trachytes typical of the 0-200 m range in the Menengai field. The loss zone at 400 m is related to the syn-caldera tuff formation, identified as one of the marker horizons in the stratigraphy. Between 700 and 1,000 m, a thick column of intermittent losses was encountered, indicating high permeability; however, no geothermal aquifer was present at this zone, based on the measured temperatures. Generally, four aquifers were mapped in this well, as described below:

Aquifer 1 is a small feed zone at 1,100 m, emanating from a lithological contact between a medium-grained and a coarse-grained trachyte. There are indications that some parts of this feed zone were cased off.

Aquifer 2 is at 1,500 m located in a tuff zone; the zone is characterised by an increase in temperature, high penetration rates and alteration.

Aquifer 3 is located in a contact zone between medium-grained trachyte and a tuff. The zone is characterised by an increase in the measured temperature, a high penetration rate and alteration.

Aquifer 4 is at 1,900 m; it is a highly altered and relatively thick tuff formation. It is characterised by a sharp inversion of the temperature profile, indicating that it is a very permeable zone and that substantial amounts of water went into the formation during drilling and is now taking a longer time to heat up. This could be the major aquifer in the well.

8. DISCUSSION AND CONCLUSIONS

8.1 Discussion

Menengai is a trachytic central volcano with a high-level magma chamber. The shallowest part of the chamber is at the summit, evidenced by the doming and recent intrusions, as seen from the analysis of cuttings from wells MW-04 and MW-05. Fresh glass is intercepted at 2,082 and 2,174 m in well MW-04 and MW-05, respectively. The cuttings were highly mixed in well MW-04, while in MW-05 the cuttings consisted of only the fresh glass and persisted for about 14 m before the drill string got stuck. Binocular and thin section analysis showed that the glass had numerous stretched vesicles and a flow of lathy texture. Such a texture is consistent with highly volatile and viscous magma. In order to better understand the chilled glass, an analysis of the volatile components, microprobe analysis and an analysis on the short lived isotopes should be done. The volatiles and microprobe analysis would help in geothermometric calculations to determine the temperature at which the magma was chilled, while the isotope analysis would help in determining its absolute age.

The geology of Menengai is divided into three stages, i.e. pre-caldera, syn-caldera and post-caldera. The identification of these stages was aided by mapping out four tuff marker horizons in the stratigraphy (Figures 10 and 20). All these stages are within the Pleistocene and Holocene epochs. The post-caldera forms the uppermost zone to about 320 m and hosts the shallow underground water aquifers, while the syn-caldera is marked by a tuff marker horizon between 320 and 400 m. The pre-caldera forms the longest column in the stratigraphy and hosts the reservoir. It is predominantly trachytic but tuff layers are also encountered. Tectonic structures in Menengai are not well understood because the caldera is heavily covered with the Holocene volcanics. However, observations at the caldera walls showed that several faults associated with the Solai system cut through the caldera rim and are, therefore, younger than the caldera. The Ol'rongai system on the other hand is older than the Solai system and is associated with the strike direction of the pre-caldera shield.

Hydrothermal minerals are mainly present in veins, vesicles and as replacements of primary minerals in the volcanic rocks. Their distribution is a pro-grade variation observed in other geothermal fields. Hydrothermal alteration minerals include: chalcedony, actinolite, pyrite, illite, pyrrhotite, wollastonite, albite, quartz and epidote. Epidote is, however, very rare probably due to high CO_2 experienced in this field or because it is not in equilibrium with the fluid chemistry. The relationship between alteration mineral and fluid chemistry is not, however, very straightforward. High CO_2 is an inhibitor to the formation of calcium bearing minerals like actinolite, wollastonite and epidote due to its affinity to Ca^{2+}. The presence of these minerals, therefore, indicates that the high CO_2 influx is a later event, most likely related to recent magmatic activity and a degassing shallow magmatic intrusion. Another probable

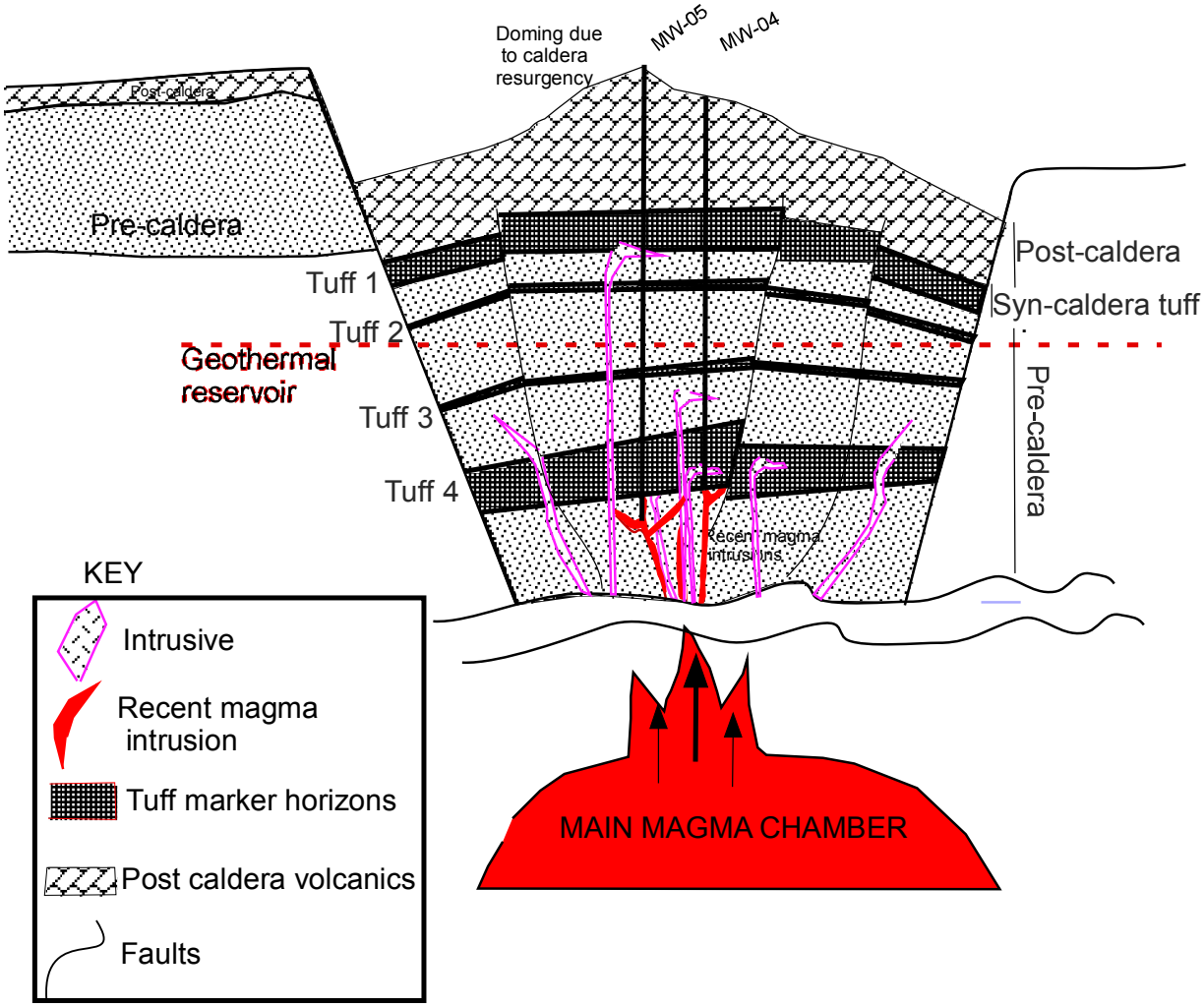

FIGURE 20: Menengai stratigraphic model

reason for epidote being rare is that Menengai geothermal system is very young geologically and that the mineral has not had enough time to form.

The inferred alteration temperature at reservoir depth is between 200 and 280°C. This is based on the occurrence of illite, wollastonite and actinolite. Based on hydrothermal alteration, the reservoir is divided into three parts: the upper and middle parts are marked by temperature ranges between 200 and 270°C, while the deeper part showed temperatures of over 280°C. These reservoir divisions correlate with: hydrothermal zone (2), the illite-quartz zone; zone (3), the illite-quartz-wollastonite zone; and zone (4), the wollastonite-actinolite zone. Homogenization temperatures (Th) in fluid inclusions of quartz and calcite are known to be particularly reliable proxies of past subsurface temperature conditions. In this study, resulting temperatures from fluid inclusions in quartz generally ranged from 180-270°C. The (Th) values at 1,500 m in well MW-04 range between 180-240°C with an average value of 240°C. In well MW-05 at 1,500 m, the (Th) values from quartz inclusions ranged from 180-270°C with an average value of 245°C. These results shows a slightly lower temperature from the fluid inclusions compared to the alteration temperatures and measured temperatures, therefore, the system is most likely heating up.

8.2 Conclusions

1. The lithology at the Menengai caldera summit is predominantly composed of trachytes with varying textures, reflecting different eruption episodes. Four tuff marker horizons were identified; the first marker was related to syn-caldera activity.

2. Sources of permeability in Menengai geothermal field are fractures and faults in the trachytes, lithological contacts between formations, and permeable tuffs.

3. Indicators of high permeability in Menengai are: high alteration intensity, high oxidization marking lithological contacts, the occurrence of abundant pyrite, calcite and loss of circulation. Low permeability, on the other hand, is indicated by low alteration and low penetration rates.

4. Hydrothermal alteration mineral assemblages in Menengai are controlled by temperature; however, the rock chemistry and fluid chemistry appear to have substantial influence.

5. Four hydrothermal zones are recognized in Menengai, the zeolite-smectite zone, the illite-quartz zone, the Illite-quartz-wollastonite zone and the wollastonite-actinolite zone.

6. Temporal changes have occurred around wells MW-04 and MW-05. The system is currently heating up, based on high alteration temperatures compared to the fluid inclusions and the anomalously high measured temperatures. The heat up could be attributed to recent magmatic intrusions in the area.

7. There is a high likelihood that some feed zones in wells MW-04 and MW-05 might have been cased off. Therefore, there is a need to consider casing programmes for wells on an individual basis.

ACKNOWLEDGEMENTS

I wish to acknowledge my employer, the Geothermal Development Company - GDC, and its Chief Executive Officer, Dr Silas Simiyu, for giving me the opportunity to attend this course. My great and sincere gratitude to the Government of Iceland, Dr. Ingvar Birgir Fridleifsson, Director, and Mr. Lúdvík S. Georgsson, Deputy director, of the United Nations University Geothermal Training Programme (UNU-GTP) for offering me admission and a chance to take part in this immensely vital course. To the UNU-GTP staff, I cannot forget Ms. Thórhildur Ísberg, Ms. Málfrídur Ómarsdóttir, Mr. Ingimar G. Haraldsson and Mr. Markús A.G. Wilde; your assistance in your respective capacities is highly appreciated. Special thanks to my supervisors: Ms. Anette K. Mortensen and Dr. Björn S. Hardarson, for their support and guidance in this project work. My deep and sincere gratitude to the entire Iceland GeoSurvey (ÍSOR) staff, in particular Dr. Hjalti Franzson, Mr. Gudmundur Gudfinnsson, Steinthór, Signý, Sigurdur and not forgetting Dr. Gudmundur Ómar from HS Orka, for taking time off from their busy schedules to share their skills and knowledge with me.

I appreciate my family and friends back home in Kenya for their encouragement and prayers. My deepest appreciation goes to my wife, Elizabeth, for her sacrifice and support, and my daughter, Precious Chebet Kiptoo, who was born while I was away. This project is dedicated to her. Thank you all, 2012 UNU fellows, for memorable moments shared during the entire period; it was a pleasure meeting and interacting with each and every one of you. The borehole geology class 2012: you are the best.

Finally, I thank God for his divine favour and the fare he has brought me.

REFERENCES

BGR, 2009: Geothermal exploration at Menengai-Ol'banita prospect. BGR, Germany, website: *www.bgr.bund.de.*

Danielsen, E.P., 2010: Servicing geothermal wells during completion and follow-up monitoring. *Proceedings of the World Geothermal Congress 2010, Bali, Indonesia*, 6 pp.

Franzson, H., 1998: Reservoir geology of the Nesjavellir high-temperature field in SW-Iceland. *Proceedings of the 19th Annual PNOC-EDC Geothermal Conference, Manila,* 13-20.

GDC, 2010: *Menengai geothermal prospect, an investigation for its geothermal potential.* GDC, Kenya, Geothermal Resource Assessment Project, unpubl. report.

Geotermica Italiana Srl., 1987: *Geothermal reconnaissance survey in the Menengai- Bogoria area of the Kenya Rift Valley.* UN (DTCD)/GOK.

Griffith, P.S., 1977: *The geology of the area around Lake Hannington and the Perkerra river, Rift Valley Province, Kenya*. University of London, PhD thesis, London, 187 pp.

Griffith, P.S., 1980: Box fault systems and ramps: A typical association of structures from the eastern shoulder of the Kenya rift. *Geol. Mag., 117,* 579-586.

Griffith, P.S., and Gibson, I.L., 1980: The geology and the petrology of the Hannington trachyphonolite formation, Kenya Rift Valley. *Lithos, 13,* 43-53.

Henley, R.W., and Ellis, A.J., 1983: Geothermal systems ancient and modern: A geochemical review. *Earth Sci. Rev., 19*, 1-50.

Jones, W.B., 1985: Discussion on geological evolution of trachytic caldera and volcanology of Menengai volcano, Rift Valley, Kenya. *J. Geol. Soc. Lon., 142*, 711 pp.

Jones, W.B., and Lippard, S.J., 1979: New age determination and Geology of Kenya rift – Kavirondo rift junction, west Kenya. *J. Geol. Soc. Lond., 136*, 63 pp.

Karingithi, C.W., Arnórsson, S., Grönvold, K., 2010: Processes controlling fluid compositions in Olkaria geothermal system, Kenya. *J. Volc. & Geoth. Res., 196*, 57-76.

KenGen, 2004: *Menengai volcano: Investigations for its geothermal potential*. KenGen, Kenya, Geothermal Resource Assessment Project, unpubl. report.

Kipng'ok, J.K., 2011: Fluid chemistry, feed zones and boiling in the first geothermal exploration well at Menengai, Kenya. Report 15 in: *Geothermal training in Iceland 2011*. UNU-GTP, Iceland, 281-302.

Koestono, H., 2007: *Borehole geology and hydrothermal alteration of well HE-24, Hellisheidi geothermal field, SW-Iceland*. Report 10 in: *Geothermal training in Iceland 2007*. UNU-GTP, Iceland, 199-224.

Lagat, J.K., 1995: *Borehole geology and hydrothermal alteration of well OW-30, Olkaria geothermal field Kenya. R*eport 6 in: *Geothermal training in Iceland 1995*. UNU-GTP, Iceland, 135-154.

Lagat, J.K., 2008: Hydrothermal alteration mineralogy in geothermal fields with case examples from Olkaria Domes geothermal field Kenya. *Paper presented at "Short Course III on Exploration for Geothermal Resources", organized by UNU-GTP and KenGen, Lake Naivasha, Kenya,* 27 pp.

Leat, P.T., 1984: Geological evolution of the trachytic caldera volcano Menengai, Kenya Rift Valley. *J. Geol. Soc. London, 141*, 1057-1069.

Leat, P.T., 1991: Volcanological development of Nakuru area of the Kenyan rift valley. *J. Afric. Earth Sci., 13*, 483-498.

McCall, G.J.H., 1967: *Geology of the Nakuru-Thomson's Falls-Lake Hannington area.* Geological Survey of Kenya, report 78, 122 pp.

Nelson, S.A., 2011: *Volcanic land forms, volcanoes and plate tectonics*. Tulane University, New Orleans, LA, website: *www.tulane.edu/~sanelson/geol204/volclandforms.pdf.*

Reyes, A.G., 2000: *Petrology and mineral alteration in hydrothermal systems. From diagenesis to volcanic catastrophes.* UNU-GTP, Iceland, report 18-1998, 77 pp.

RockWare, 2007: *LogPlot program.* RockWare, Inc., USA.

Simiyu, S.M., 2009: Application of micro-seismic methods to geothermal exploration: Examples from Kenyan rift. *Paper presented at "Short Course V on Exploration for Geothermal Resources", organized by UNU-GTP, GDC and KenGen, at Lake Naivasha, Kenya,* 27 pp.

Thompson, A.J.B., and Thompson, J.F.H. (editors), 1996: *Atlas of alteration: A field and petrographic guide to hydrothermal alteration minerals*. Alpine Press Ltd., Vancouver, British Columbia, 119 pp.

APPENDIX I: Stratigraphy of the Central Kenyan Rift Valley

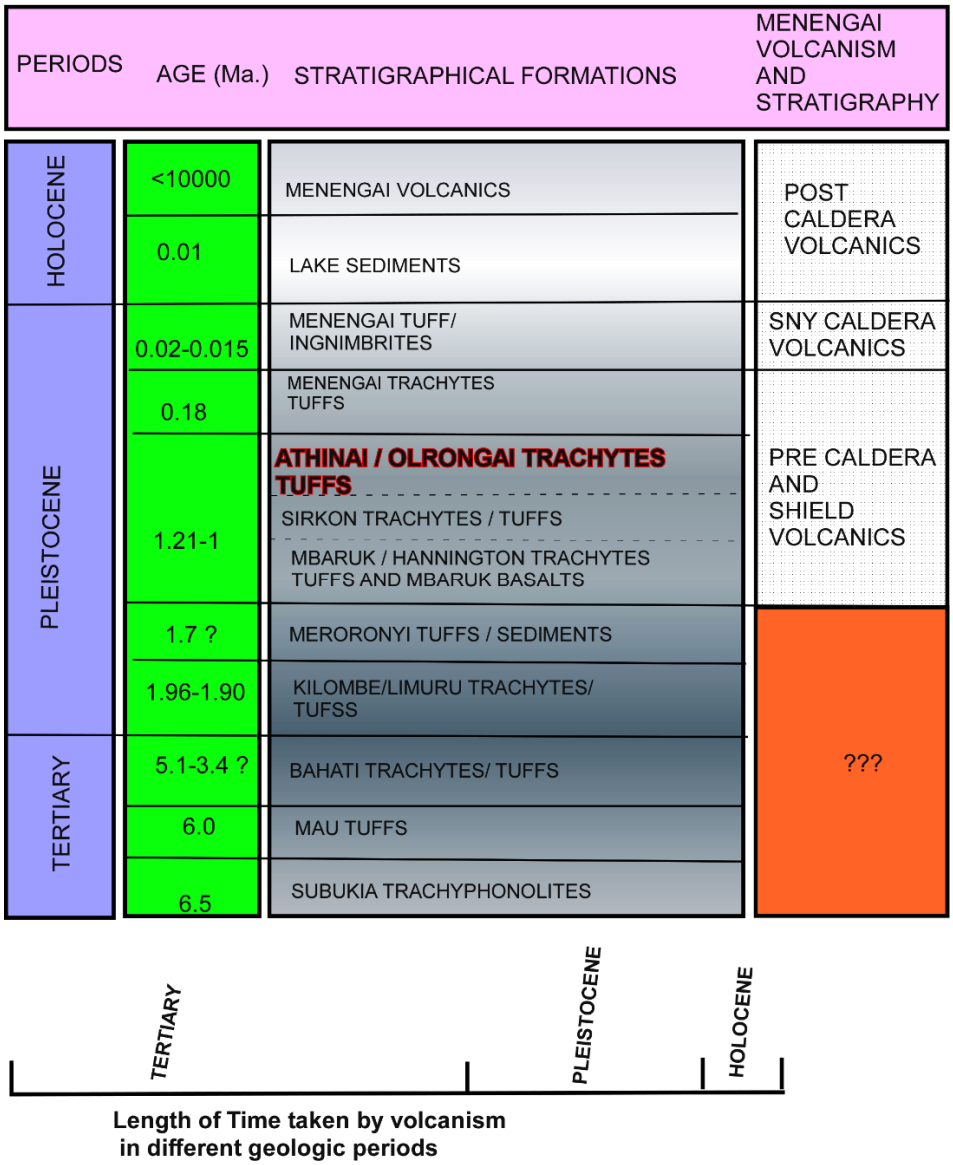

FIGURE 1: General stratigraphy and volcanology of Kenyan Central Rift Valley in reference to Menengai Volcano

APPENDIX II: Chemical formulae of some alteration minerals in Menengai

Name	Chemical formulae
Epidote (Rare)	$Ca_2Al_2(Fe^{3+};Al)(SIO_4)(Si_2O_7)O(OH)$
Wollastonite	$CaSiO_3$
Albite	$NaAlSi_3O_8$
Adularia	$KAlSi_3O_8$
Actinolite	$Ca_2(Mg,Fe)_5Si_8O_{22}(OH)_2$
Cowlescite	$CaAl_2Si_3O_{10}.6(H_2O)$
Pyrite	FeS_2
Quartz	SiO_2
Chalcedony	SiO_2
Opal	$SiO_2.nH_2O$
pyrrhotite	Fe_nS
scolecite	$Ca_2Al_2Si_3O_{10}.3H_2O$
mesolite	$Na_2Ca_2(Al_2Si_3O_{10})_3.3H_2O$

APPENDIX III: List of XRD analyses

Feldspars and amphiboles mentioned are primary minerals

Id	Well MW-04		Well MW-05	
	Depth (m)	Remark	Depth (m)	Remark
1	192-194	Smectites, zeolite, feldspars	216-218	Amphiboles
2	244-246	Smectites, zeolite, feldspars	326-328	Amphiboles, feldspars
3	362-364	Illite zeolites	334-336	Smectites, illite, zeolite, feldspars
4	586-588	Feldspars	414-416	Amphiboles, feldspars
5	690-692	Feldspars	552-554	-
6	804-806	Smectite, feldspars	684-686	smectites
7	950-952	Smectite, feldspars	786-788	Smectite, illite
8	1068-1070	Feldspars	834-836	Smectite, illite
9	1186-1188	Amphiboles, feldspars	910-912	Smectite, illite
10	1288-1290	-	994-996	Smectite, amphiboles, feldspars
11	1426-1428	Trace illite, amphiboles	1110-1112	Smectites, illite, amphiboles
12	1584-1586	Illite amphiboles feldspars	1238-1240	Amphiboles, feldspars
13	1762-1764	Illite amphiboles feldspars	1496-1498	-
14	1788-1790	Illite amphiboles feldspars	1564-1566	Illite, amphiboles, feldspars
15	1886-1888	Trace illite	1628-1630	Illite, feldspars
16	1956-1958	Illite, amphiboles	1668-1670	Illite, amphiboles
17	2032-2034	Amphiboles	1684-1686	Illite, amphiboles
18	2094-2096	Amphiboles	1800-1802	Illite, amphiboles

APPENDIX IV: Typical diffractograms of smectites, zeolites and illite clays from Menengai

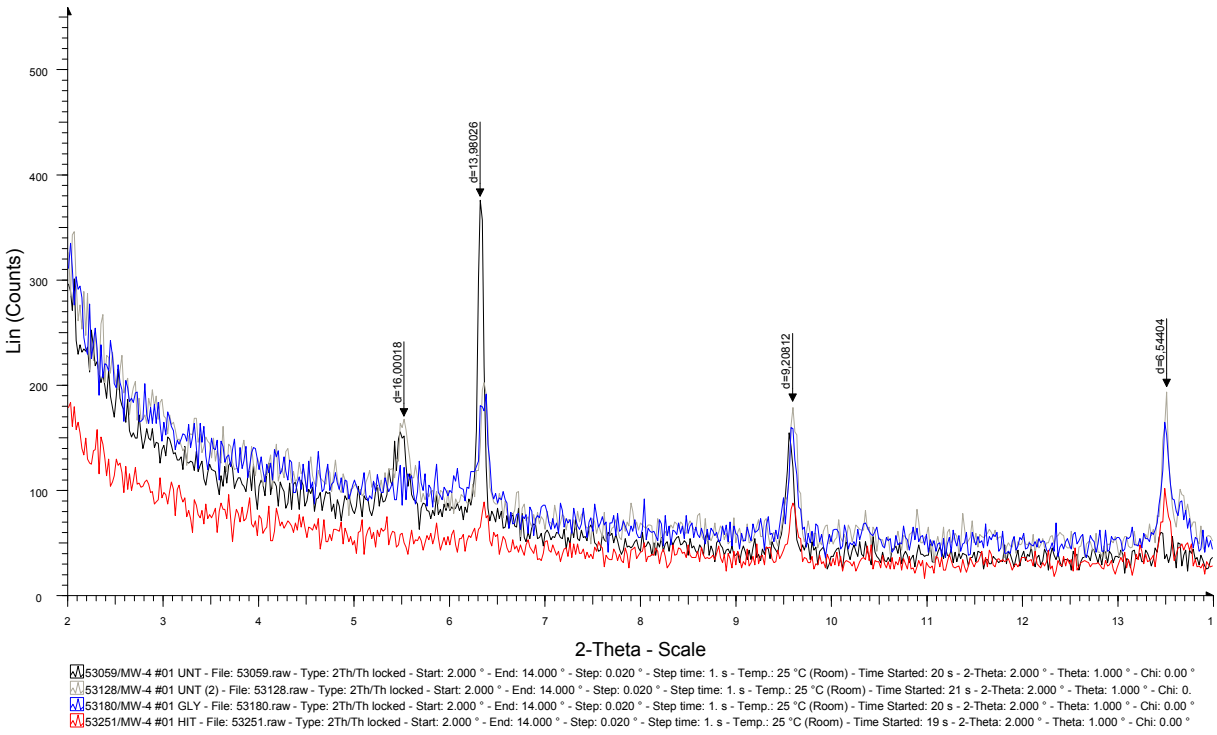

FIGURE 1: Well MW-04 Menengai, XRD analysis of sample 1

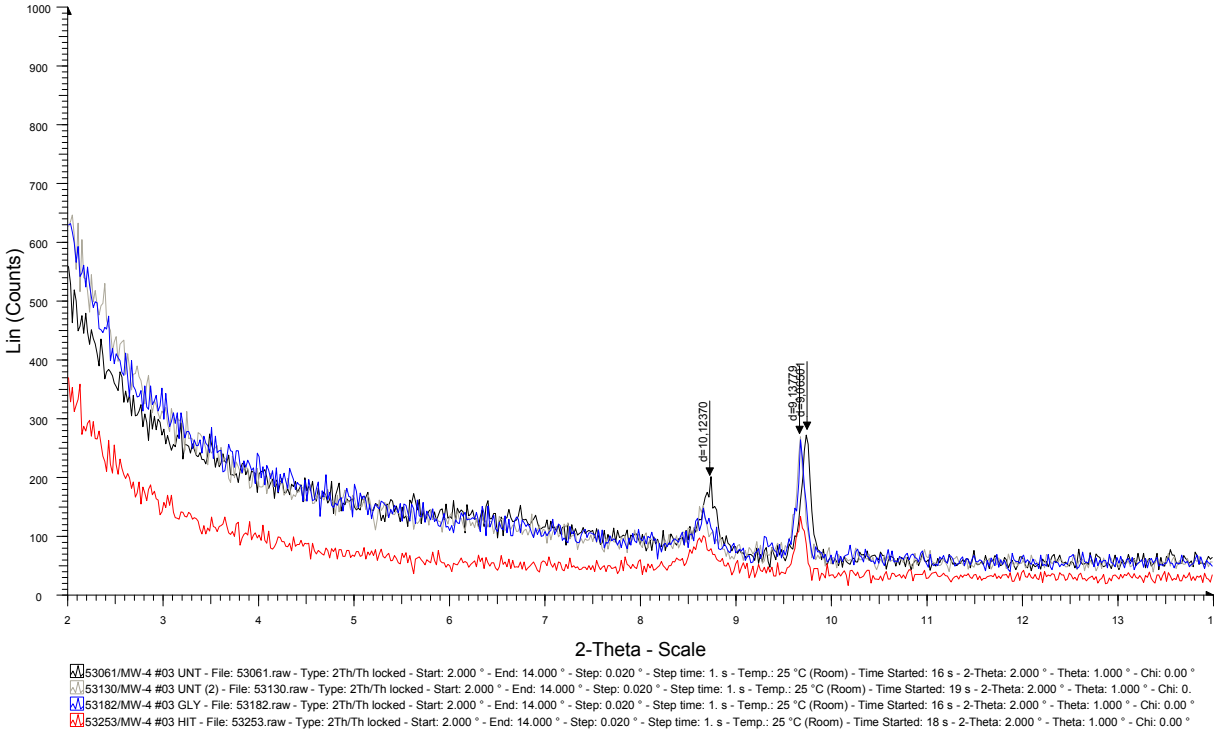

FIGURE 2: Well MW-04 Menengai. XRD analysis of sample 3